Faculteit Industriële Ingenieurswetenschappen

master in de industriële wetenschappen: elektronica-ICT

Masterthesis

Development of biopotential amplifier for ECG, EEG, EMG and EOG for educational purposes

Sam Beuk

Scriptie ingediend tot het behalen van de graad van master in de industriële wetenschappen: elektronica-ICT

PROMOTOR :
ing. Thijs VANDENRYT

PROMOTOR :
Prof. dr. Roca GONZÁLEZ

Gezamenlijke opleiding UHasselt en KU Leuven

UHASSELT KU LEUVEN

Universiteit Hasselt | Campus Diepenbeek | Faculteit Industriële Ingenieurswetenschappen | Agoralaan Gebouw H - Gebouw B | BE 3590 Diepenbeek

Universiteit Hasselt | Campus Diepenbeek | Agoralaan Gebouw D | BE 3590 Diepenbeek
Universiteit Hasselt | Campus Hasselt | Martelarenlaan 42 | BE 3500 Hasselt

UHASSELT KU LEUVEN

2022
2023

Faculteit Industriële Ingenieurswetenschappen

master in de industriële wetenschappen: elektronica-ICT

Masterthesis

Development of biopotential amplifier for ECG, EEG, EMG and EOG for educational purposes

Sam Beuk

Scriptie ingediend tot het behalen van de graad van master in de industriële wetenschappen: elektronica-ICT

PROMOTOR :

ing. Thijs VANDENRYT

PROMOTOR :

Prof. dr. Roca GONZÁLEZ

UHASSELT KU LEUVEN

Foreword

This thesis was written for the Master's degree of industrial engineering electronics and ICT. I wrote this thesis while being on an exchange in Cartagena, Spain. Beside the many cultural experiences I had the privilege of immersing myself in, I enjoyed working with the people and forming connections that I will cherish for the rest of my life. This research has also improved my general understanding of analog circuitry and biomedical engineering. My hope is that this research will help future biomedical engineering students learn the working of biopotential amplifiers as well as the analysis of the electrograms.

First of all, I want to thank Prof. Dr. Roca González for his guidance and recommendations during the development and testing of the biopotential amplifier. I also want to thank my promoter ing. Thijs Vandenryt for his helpful insights, reviews and general guidance from a long distance. They both helped me grow a lot in my understanding of electronic engineering with their expertise.

Table of contents

Foreword 1
List of tables 5
List of figures 7
Abstract (English) 9
Abstract (Nederlands) 11
1 Introduction 13
1.1 Measured signals 13
1.1.1 (Surface) Electromyography 13
1.1.2 Electrocardiogram 14
1.1.3 Electrooculogram 15
1.1.4 Electroencephalogram 15
1.2 Powerline interference 15
1.3 Common mode rejection ratio 16
1.4 Input impedance 17
2 Proposed amplifier 19
2.1 Input stage 19
2.1.1 Instrumentation amplifier 19
2.1.2 AC-coupling network 21
2.2 DC restoration 23
2.3 Driven Right Leg 23
2.4 Low pass filter 24
3 Materials 27
3.1 Requirements 27
3.2 Bio simulator 27
3.3 Electrodes 28
3.4 Output of the amplifier 29
3.5 Simulation software 30
3.6 Electrical characteristics of circuit based on signal 31
3.7 Overview of total circuit 32
3.8 AC-coupling network 32
3.9 Instrumentation amplifier 34
3.10 DC restoration 35
3.11 Driven Right Leg 37
3.12 Low pass filter 38
3.13 Operational amplifier 40

4 Results 41
4.1 Simulations 41
4.1.1 Electrocardiogram 41
4.1.2 Electromyography 42
4.1.3 Electrooculogram 43
4.1.4 Electroencephalogram 43
4.2 Prototype design 44
4.2.1 Basic design 44
4.2.2 Configurable design 46
4.2.3 Combined design 49
4.3 Powerline interference 49
4.4 Bio simulator test 50
4.4.1 Pre-testing 50
4.4.2 Biopac MP35 52
4.5 Test subject 53
4.5.1 Electromyography 53
4.5.2 Electrocardiogram 55
4.5.3 Electrooculogram 57
5 Discussion of results 59
5.1 Simulations 59
5.2 Bio simulator test 59
5.3 PCB prototype design 59
5.3.1 Proposed adjusted design 60
5.4 Test subject 61
6 Conclusion 63
Bibliography 65
Appendices list 67
Appendices 69

List of tables

TABLE 1: ELECTRICAL CHARACTERISTICS OF ECG, EMG, EEG AND EOG. UPPER AND LOWER FREQUENCY (IN HZ) AND THE AMPLITUDE (IN μV) 31
TABLE 2: THE DIFFERENT UPPER CUT-OFF FREQUENCIES FOR EACH ELECTROGRAM, WITH THE SELECTED FEEDBACK RESISTANCE 39

List of figures

Figure 1: Typical ECG signal with a P wave, QRS complex and T wave. The U wave has a small size and is not always seen on an ECG 14
Figure 2: ECG signal affected by powerline interference 16
Figure 3: Simplified block diagram overview of the circuit 19
Figure 4: Standard instrumentation amplifier with output voltage formula 20
Figure 5: AC coupled networks. a) passive differential high pass filter in front of a DC-amplifier b) Fully differential passive AC-coupling network built by mirroring two single-ended, high-pass filters whose common node is connected to the common-mode input voltage obtained through an ungrounded passive voltage adder 22
Figure 6: Graph displaying CMRR (dB) on y-axis in function of frequency (Hz) on x-axis. Used network (network 3) compared with the other networks 22
Figure 7: DC restoration circuit, an integrator in feedback loop around difference amplifier 23
Figure 8: Bode-diagram of second order system with different damping coefficients and cut-off frequency (w_N = 1, K =1) 25
Figure 9: Bio simulator that generates an ECG signal 28
Figure 10: Medical electrode adapter to 3.5 mm jack 29
Figure 11: Biopac MP35. A data acquisition system with four channels 30
Figure 12: Overview of the proposed circuit for the bio amplifier 32
Figure 13: a) AC-coupling circuit with no source impedance b) AC transfer characteristics frequency response simulation with the gain on the y-axis in dB and the frequency on the x-axis in Hz. The red line is at 0.05 Hz and -1,65 dB. Blue line is on 0,034 Hz and -3 dB 33
Figure 14: DC transfer characteristics where the output voltage (in V) on the y-axis is in function of source resistance (in Ω) on the x-axis 34
Figure 15: Stage 1 of the instrumentation amplifier, gain is set at 1001. On the right is the AC frequency response of the circuit with the gain (dB) on the y-axis and the frequency (Hz) on the x-axis 35
Figure 16: On the left the circuit of an integrator in a feedback loop around the difference amplifier. On the right the AC frequency response of this circuit with the gain (dB) on the y-axis and the frequency (Hz) on the x-axis. The red line is set at 0.05 Hz with an amplitude of -0.49 dB. The blue line is set at the cut-off frequency, -3 dB, at 0.0164 Hz 36
Figure 17: Left: The DC restoration circuit combined with the AC-coupling network and the instrumentation amplifier. On the right the AC frequency response for A_{v0} = 1001 and R_i = 10 MΩ with the gain (dB) on the y-axis and the frequency (Hz) on the x-axis. The red line at 0.05 Hz has a gain of 57.79 dB. The blue line has a gain of 57 dB at 0.04 Hz 37
Figure 18: Used driven right leg circuit 38
Figure 19: Left: AC frequency response of driven right leg circuit with a C_{DRL} of 10nF. Right: The AC frequency response of the driven right leg circuit with no C_{DRL}. For both graphs the gain (dB) on the y-axis and the frequency (Hz) on the x-axis 38
Figure 20: Second order Sallen key Low pass filter. On the right the AC frequency response with the gain (dB) on the y-axis and the frequency (Hz) on the x-axis. The blue line is at 150 Hz with a gain of -5.56 dB 39
Figure 21: The circuit that is built in TINA-TI. This example has the configurations for an ECG 41
Figure 22: AC frequency response of the electrocardiogram displaying the gain (dB) and phase change (degrees) in function of the frequency in Hz. Red line (a) is at 0.05 Hz at a gain of 57.8 dB. The blue line (b) is at 150 Hz and has a gain of 54.3 dB 42
Figure 23: AC frequency response of the electromyography displaying the gain (dB) and phase change (degrees) in function of the frequency in Hz. Red line (a) is at 20 Hz at a gain of 57.8 dB. The blue line (b) is at 500 Hz and has a gain of 52.6 dB 42
Figure 24: AC frequency response of the electrooculogram displaying the gain (dB) and phase change (degrees) in function of the frequency in Hz. Red line (a) is at 0.05 Hz at a gain of 57.7 dB. The blue line (b) is at 10 Hz and has a gain of 54.3 dB 43
Figure 25: AC frequency response of the electroencephalogram displaying the gain (dB) and phase change (degrees) in function of the frequency in Hz. Red line (a) is at 0.05 Hz at a gain of 63.7 dB. The blue line (b) is at 40 Hz and has a gain of 59.9 dB 44

Figure 26: KiCad schematic of the basic design 45
Figure 27: PCB design of the basic prototype without ground plane 46
Figure 28: KiCad schematic of the configurable circuit 47
Figure 29: The PCB design for the configurable design without a ground plane 48
Figure 30: Configurable design with all components soldered. The jumpers are configured to receive an ECG signal through the mini jack 48
Figure 31: Final prototype design, the two designs combined onto one board 49
Figure 32: Powerline interference of 200 mV at 50 Hz when the oscilloscope is connected to the PCB. The PCB is connected to a 5 V power supply that is not delivering power at the moment of this picture 49
Figure 33: Output of the bio simulator on an oscilloscope without the usage of the bio simulator 50
Figure 34: The signal of the bio simulator amplified by the designed biopotential amplifier received by an analog input of the Arduino Uno. The amplitude (mV) on the y-axis and the time (ms) on the x-axis 51
Figure 35: The output of the bio simulator with a gain of 92. The amplitude (mV) on the y-axis and the time (ms) on the x-axis. The left graph has 500 mV/division while the right picture has 200 mV/division with an offset of 1.25V 51
Figure 36: The amplified ECG signal with a horizontal scale of 100 ms/division and a vertical scale of 200 mV/division. The left graph is a sample, the right graph uses averaging 52
Figure 37: Amplification of bio simulator by the biopotential amplifier with a gain of 400. The amplitude (mV) on the y-axis and the time (seconds) on the x-axis. No digital filters are applied 53
Figure 38: Position of electrodes placed on the bicep for an electromyography 54
Figure 39: The graph of EMG output with the amplitude (mV) on the y-axis and the time (seconds) on the x-axis. The red (top) graph is the raw EMG signal measured from the bicep and in blue (bottom) the RMS and average filtered per 40 samples with sample rate of 1000 samples per second. A digital 50 Hz stop band filter is applied. The duration of the measurement is 50 seconds. 55
Figure 40: Electrode placement for an electrocardiogram 55
Figure 41: Heart signal amplified by 1001, no band pass filter applied from the Biopac MP35. The amplitude (mV) on the y-axis and the time (seconds) on the x-axis 56
Figure 42: Heart signal amplified by 1001 with an electronic device close to the PCB. The amplitude (mV) on the y-axis and the time (seconds) on the x-axis 56
Figure 43: Heart signal amplified by 1001 with the usage of Biopac MP35 band stop filter at 50 Hz. The amplitude (mV) on the y-axis and the time (seconds) on the x-axis 57
Figure 44: Electrooculogram of horizontal view. The amplitude (mV) on the y-axis and the time (seconds) on the x-axis. The test subject looks to the right at beginning of the measurement, followed by looking forward, then left. The measurement finishes after blinking the eyes repeatedly 58
Figure 45: Electrical schematic of the improved PCB design 60
Figure 46: PCB design of the improved board 61

Abstract (English)

Electrical signals play a crucial role in various activities of the human body. Measuring electrical potential differences can give insight into the functioning of different body parts. In this work, the authors focus on electrocardiography (ECG), electromyography (EMG), electrooculogram (EOG), and electroencephalogram (EEG). After data collection, the signals are conditioned with a biopotential amplifier. The biomedical engineering department of the Polytechnic University of Cartagena needed an accurate, robust, and low-cost amplifier that can perform the mentioned electrograms. To realize this, an instrumentation amplifier is selected as the core element. This amplifier is paired with additional circuitry to filter out noise, improve electrical isolation, defibrillation shock protection, adding a known DC offset and a gain of the differential signal while being powered by a single supply. After simulations of the amplifier, a prototype was designed and built onto a printed circuit board. This device can accept the biopotentials from a simulator or via a 3.5 mm jack. Configuration of the bandwidth and gain can be performed by changing the position of jumpers. The device was first validated with a biopotential simulator before moving to a test subject. It successfully performed an ECG where the P wave, QRS complex, and T wave are distinguishable. Furthermore, with the EOG it is possible to tell the direction the subject is looking and the EMG can detect the usage of muscles, as expected from simulations.

Abstract (Nederlands)

Elektrische signalen spelen een cruciale rol bij verschillende activiteiten van het menselijk lichaam. Het meten van elektrische potentiaalverschillen kan inzicht geven in het functioneren van verschillende lichaamsdelen. In dit werk richten de auteurs zich op elektrocardiografie (ECG), elektromyografie (EMG), elektro-oculogram (EOG) en elektro-encefalogram (EEG). Een biopotentiaalversterker conditioneert de verzamelde signalen. De afdeling biomedische techniek van de Polytechnische Universiteit van Cartagena had een nauwkeurige, robuuste en goedkope versterker nodig die de genoemde elektrogrammen kan uitvoeren. Om dit te realiseren is gekozen voor een instrumentatieversterker als kernelement, met extra schakelingen om ruis te filteren, de elektrische isolatie te verbeteren, bescherming tegen defibrillatieschokken, het toevoegen van een bekende DC offset en een versterking van het differentiële signaal met één enkele voeding. Na simulaties van de versterker werd een prototype ontworpen en op een printplaat gebouwd. Het is mogelijk om biopotentialen te ontvangen via een simulator of 3,5 mm jack. Configuratie van de bandbreedte en versterking gebeurt door het herplaatsen van jumpers. Het apparaat werd eerst gevalideerd met een biopotentialensimulator voordat het getest werd op een proefpersoon. Het heeft met succes een ECG uitgevoerd waarbij de verschillende golven te onderscheiden zijn. Verder is het met de EOG mogelijk om de richting te bepalen waarin de proefpersoon kijkt en kan de EMG het gebruik van spieren detecteren.

1 Introduction

Electrical signals are used throughout every function or activity of the human body. A neuron is a specialized cell for the reception, interpretation and transmission of these electrical signals. These neurons carry the signals from sense organs to the central nervous system which consists of the brain and spinal cord. The signals are then analyzed and interpreted, followed by a response sent to the muscle cells and glands [1], [2].

One way of studying the human body is by measuring the potential difference between electrodes that catch electrical signals generated by the body. An electrode is a specialized sensor that is attached to the human body either invasively or as done in this thesis, non-invasively. The electrical potentials of the muscle can be seen in Electromyography (EMG), the heart in Electrocardiography (ECG), the brain in Electroencephalogram (EEG) and the potential of the eye in electrooculogram (EOG). Physicians can use these potential differences for diagnosing medical conditions of their patients [3].

The biomedical engineering department of the Polytechnic University of Cartagena needed an accurate, robust, and low-cost amplifier that can perform the different mentioned electrograms. For this reason, a biopotential amplifier circuit is designed and later built onto a printed circuit board (PCB). Its goal is to introduce students to work with an amplifier on a PCB while also using Biopac Student Lab software [4].

At its core, a biopotential amplifier consists of an instrumentation amplifier. This amplifier should have a high input impedance, high amplification and be able to reject electrical interference. Additional circuitry improves the characteristics such as electrical isolation and defibrillation shock protection that ensure the patient's safety, as well as reduce electrical interference.

The main requirements of the bio amplifier are: it has to fit on a 50 x 100 mm 2-layer PCB with low-cost components combined with reasonable accuracy. All components have to be Dual in-line Package (DIP) easily solderable.

The research phase starts with understanding the working of provided electrograms and their expected frequency and amplitude range. Secondly, the electrical circuit of the bio amplifier is separated into stages and the working of each stage is investigated. After that, the required components are calculated based on the expected input signals. Every stage of the circuit is simulated separately using these components. The stages are then joined to create the full circuit, which are then simulated to see the frequency response for each electrogram.

The electrical circuit is laid out, this design is commercially fabricated, and finally the PCB is assembled. This PCB is pre-tested on an Arduino Uno, subsequently an oscilloscope is used for precise measurements. Both by using a bio simulator at the input. The final stage in the verification tests is the Biopac MP35. After a high level of confidence in both the operation and safety has been established, a voluntary test-subject is used to record the different electrograms.

1.1 Measured signals

1.1.1 (Surface) Electromyography

Electromyography (EMG), or surface Electromyography (sEMG) in the context of this paper, is the detection and analysis of the electrical potential produced during muscle contraction.

The sEMG is a non-invasive way to detect the electrical potentials by applying electrodes on the skin. sEMG is widely used in sport science because of its non-invasive way to analyze the velocity and intensity of specific muscles. The frequency range of the EMG signal is from a few hertz to hundreds of hertz. According to [5] the frequency ranges from 6 Hz to 600 Hz with the dominant frequency between 20 Hz to 150 Hz. Other sources like [6] indicate a range between 15 Hz and 400 Hz. The amplitude of the signal depends on the intensity of the muscle contraction, but it can reach a peak to peak amplitude of 5000 µV [5].

1.1.2 Electrocardiogram

An electrocardiogram (ECG) is the graphical recording of the electrical activity in the heart. This activity can be received by electrodes placed in a non-invasive way on the skin. The recorded electrical signals make the atrial and ventricular muscles of the heart contract and relax.

The ECG signal is a medical method to examine the working of the different muscles in the heart. The heart has four chambers, the upper two are called the left and right atrium while the two chambers at the bottom are called the left and right ventricle. The voltage graph of an electrocardiogram typically has a P wave, a QRS complex followed by a T wave and a U wave as shown in figure 1. Sometimes the U wave cannot be seen due to its small amplitude, generally one fourth of the T wave.

Beside the wave amplitudes, there are the time intervals between the waves which are essential in the assessment of cardiac health. Typically, the PR-interval starts at the beginning of the P wave until the peak of the R wave. When heart disease is present, such as scarred or reddened heart tissue, the PR-interval can be longer because it takes more time for the depolarization wave to extend through the atrial myocardium and the AV node [7].

Commonly, the ECG frequency range is determined to be between 0.05 and 150 Hz. The signal has a peak-to-peak amplitude of 1000 µV to 2000 µV. The electrocardiogram suffers from 3 main sources of noise namely, the powerline interference, baseline wander and Electromyography (EMG) noise [7]–[9]. Powerline interference applies on each of the selected electrograms and is further elaborated in section 1.2.

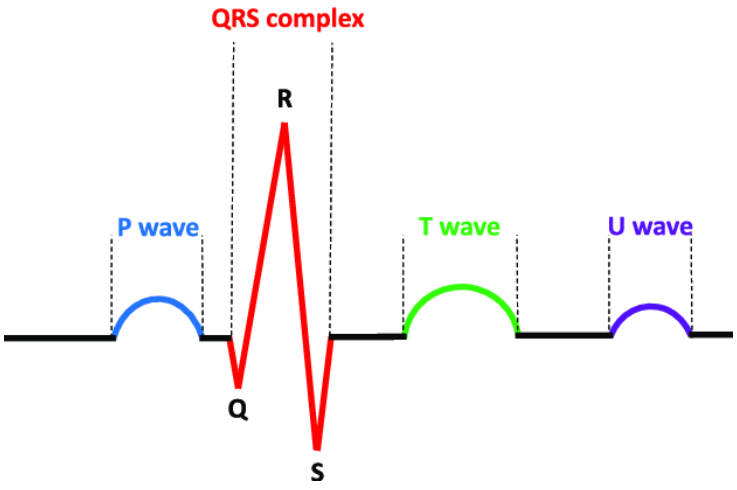

Figure 1: Typical ECG signal with a P wave, QRS complex and T wave. The U wave has a small size and is not always seen on an ECG [10]

Baseline wander is caused by patient's movement and respiration, skin-electrode impedance and poor skin-electrode contact. This results in an effect where the base axis of the signal is not horizontal, but it appears to wander, slowly moving up and down. The amplitude of the noise can easily exceed the amplitude of the QRS-complex and the frequency ranges between 0.05 and 1 Hz. The change of skin-electrode impedance appears during skin stretching due to movement of the patient.

The muscle artifacts or EMG signals represent a major problem in recordings during exercise. It can alter the shapes of the different ECG waves because of the overlapping frequency of EMG and ECG signals. This overlapping makes it hard to remove the noise because narrowband filtering cannot remove it. As the ECG signal is a repetitive signal, the muscle artifacts can be removed by an averaging over multiple heart beats [8], [9].

1.1.3 Electrooculogram

The interpretation of the electrical potential difference of the eye is called electrooculogram (EOG). There is an electrical potential between the cornea and the retina, known as the corneoretinal potential. The cornea is positioned at the front of the eye and has a positive charge while the retina is at the back of the eye and has a negative charge, creating an electric dipole. When the eye moves, the electrical dipole will move and change the electrical field around it. These changes can be detected with an EOG by placing electrodes around the eye [11].

EOG signals are band limited approximately from 0 to 50 Hz. According to [12], almost 90% of the EOG signal can be found in the range of 1 to 12 Hz. This band limit also reduces the noise generated by EEG and EMG signals, e.g., blinking and brain activity. The amplitude of the EOG is between 50 and 3500 µV.

1.1.4 Electroencephalogram

An electroencephalogram (EEG) is the recording of electrical activity of the brain. The electrical potential difference is created when neurons of the brain process information by changing the electrical current flow across membranes.

Normally, an array of electrodes is used to obtain these potential differences but in the context of this paper only 3 electrodes are available to attach to the scalp. It is still interesting to try and detect these signals to test the accuracy of this biopotential amplifier. Although the frequency of EEG signals is 0.5 Hz to 100 Hz, the most interesting components can be found below 30 Hz. Compared to ECG, EMG and EOG, the amplitude of EEG signals are low, ranging typically from 10 – 300 µV [13].

1.2 Powerline interference

Powerline interference is present during any biopotential measurement on the human body. This is the interference around the 50 Hz frequency and its harmonics. It is created by electromagnetic fields of the ac voltage line that is always present, by the medical equipment or even a light in the room. It is necessary to remove this noise because it will superimpose the low frequency waves. For example, at an Electrocardiogram (ECG) the P and T wave will not be distinguishable from the noise as seen in

figure 2 [14]. The amplifier in this thesis uses the Driven Right Leg (DRL) technique to remove the potential of the body, also called the common mode potential.

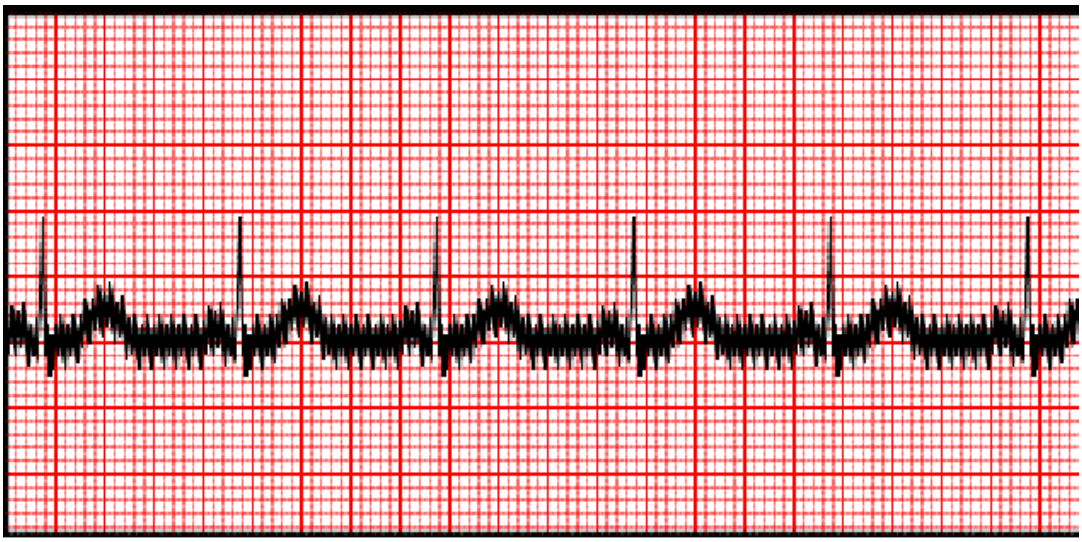

Figure 2: ECG signal affected by powerline interference [8, p. 2]

1.3 Common mode rejection ratio

The common-mode rejection ratio (CMRR) is a metric that indicates how well an amplifier rejects the common mode signal, in general the common noise and the direct current (DC) voltage. More particular for biopotential signals, the rejection of the powerline interference and the rejection of the DC offset that the biopotential signal has.

A high CMRR is necessary when large common-mode signals are present. The output voltage of a differential amplifier is given by the formula 1. This formula displays that the output of the amplifier v_0 is affected by the gain A_d times the input voltage v_{id} of the differential signal and also by the gain A_{cm} times the input voltage v_{cm} of the common mode signal. A good differential amplifier has a high CMRR which means that the gain of the differential signal is much higher than the gain of the common-mode signal. This can be derived from formula 2, which also displays that CMRR is expressed in decibels. In this formula, 20 times the logarithm with base 10 is taken of the differential gain A_d divided by the common mode gain A_{cm}.

$$v_o = A_d v_{id} + A_{cm} v_{icm} \quad (1)$$

$$CMRR = 20\, log \frac{|A_d|}{|A_{cm}|} \quad (2)$$

1.4 Input impedance

The input impedance of the biopotential amplifier is an important design criterion. If the input impedance of the amplifier is much higher than the internal impedance of the source, the voltage between the two input terminals is nearly the same as the internal source voltage.

The biopotential differences generated throughout the human body are caught by electrodes placed on the skin. If the human body is seen as the source of these potential differences, then the impedance of the skin can be seen as the source impedance of the input signal. For this reason, the skin should be prepared before applying the electrodes to make sure the contact is optimal and therefore the impedance minimal. Still, the impedance between the electrodes and the skin is different from person to person and can be high. Therefore, according to [15], the input impedance of an ECG amplifier should be larger than 2.44 MΩ.

To calculate the actual voltage at the input terminals, the Thévenin resistance of the source and of the input terminals is filled in formula 3 [16, p. 457].

$$V_{in} = V_{source} \frac{R_{in}}{R_{source}+R_{in}} \tag{3}$$

For example, if the skin impedance would be 10 kΩ, the signal 10 V and the input impedance is 100 kΩ the signal at the input terminals will be

$$Input\ V = 10\ V * \frac{100k\Omega}{10\ k\Omega + 100\mathrm{k}\Omega} = 9.09\ V$$

If the input impedance is 1 MΩ the input signal will be

$$Input\ V = 10\ V * \frac{1\ M\Omega}{10\ k\Omega + 1\mathrm{M}\Omega} = 9.90\ V$$

This example shows the importance of a high input impedance of the biopotential amplifier as well as a low impedance between the skin and electrode.

2 Proposed amplifier

The proposed amplifier used in this paper is based on the ac-coupled biopotential amplifier from Spinelli et al. [15]. The simplified version of this circuit is shown in figure 3. This amplifier is selected because of its high gain while using a reduced number of low-cost parts, resulting in low power consumption. Its proposed AC-coupling stage does not use a grounding resistor which gives it an overall high CMRR. Lastly, with the reference voltage connected to non-inverting input of the operational amplifier (op amp) in the Driven Right Leg Circuit and to op amp of the DC restoration circuit, single-supply operation of the amplifier is possible.

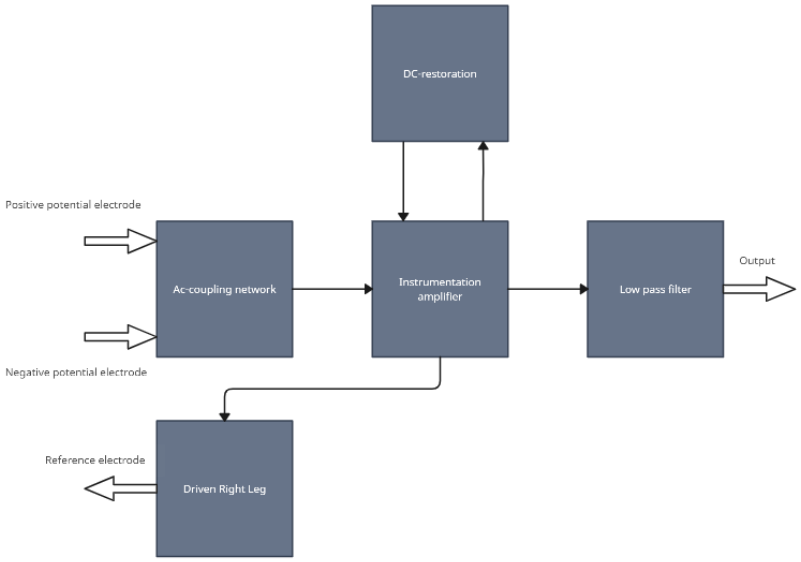

Figure 3: Simplified block diagram overview of the circuit

2.1 Input stage

The electrical signal from the patient's body contains an AC-signal superimposed on a larger DC voltage. The useful information can only be found in the AC-signal, therefore it is necessary to remove the common-mode noise and the DC voltage to be able to examine the relevant information in the signal. To remove these unwanted voltages, an ac-coupled network should be placed before a differential amplifier.

2.1.1 Instrumentation amplifier

An instrumentation amplifier is an improved differential amplifier circuit compared to a single differential amplifier. It has the combination of high CMRR, high input impedance and high gain if required. As shown in figure 4, it consists of multiple differential amplifiers, three in this case, combined with high-precision resistors, and at the end a single ended output. Both input signals are connected to the non-inverting inputs of the first two differential amplifiers. They have a negative feedback connection via resistor R_f. The inverting inputs are also connected by the gain-setting resistor R_g.

The CMRR of an instrumentation amplifier is not dependent on the internal resistances of the source. This is ideal for the application where electrodes need to be connected to the human skin. The skin should be prepared before applying the electrodes to make sure the contact is optimal. However, the impedance of the skin will change during the measurements due to transpiration, stretching, during movements or due to other factors. The independence of the source resistance is possible because of the summing-point constraint at the inputs of the differential amplifiers X_1 and X_2. The summing-point constraint is the assumption that the input voltage and current are zero, for an ideal op amp. However, these are not ideal op amps but the input current from the source will be close to zero because of the high input impedances. This makes the resistor matching not as critical as it would be for a single differential amplifier, reducing the cost of the amplifier [16].

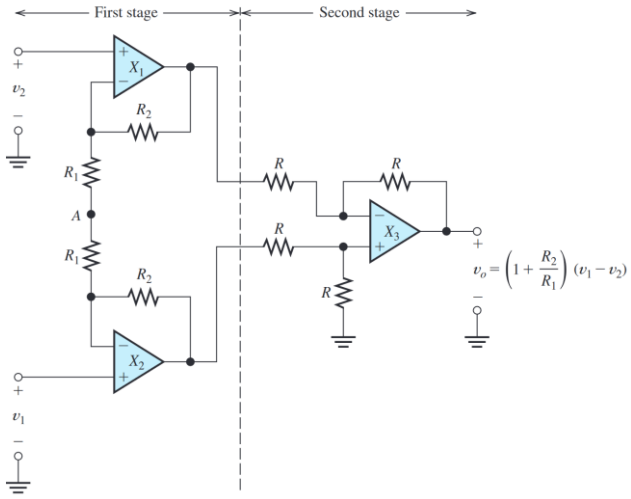

Figure 4: Standard instrumentation amplifier with output voltage formula [16, p. 697]

The instrumentation amplifier has a higher gain for a differential signal than for a common-mode signal in the first stage. If v_2 at the non-inverting input of X_1 is the exact opposite of the signal at the non-inverting input of X_2 ($v_1 = -v_2$) then the voltage in point A will be zero because the circuit is symmetrical. There will be a voltage drop across resistor R1 equal to the voltage difference between inputs V1 and V2. If the input source is a common-mode signal ($v_1 = v_2$), the voltage between the input terminals will be zero because of the summing-point constraint. Thus, the voltages at the inverting input terminals will both be v_{cm}. Therefore, no current flows through R_f and R_g resistors and the output of the amplifier is equal to v_{cm} [17].

In other words, the gain in differential mode is equal to $A_{V0} = (1 + R_f/R_g)$ and the common-mode gain is 1 or unity, for the circuit displayed in figure 4. If the circuit has only one gain resistor, the formula changes to $A_{V0} = (1 + 2R_f/R_g)$. However, as will be explained in chapter 2.3, there is a need for two resistors to use a driven right leg.

The gain for a differential mode and unity for common mode results in a high CMMR for the input stage of the instrumentation amplifier. The higher the gain in this stage, the higher the CMMR will be. The gain however, is limited to the supply rail of the op amp [18]. The output voltage should be limited so:

$$V_{CM} \pm 0.5V_{diff}(1 + R_f/R_g) < V_{supply\ rail} \quad (4)$$

The symmetrical matched R_f's do not require precise matching. Mismatched feedback resistors still have unity gain in common-mode and the differential gain changes to $A_{V0} = 1 + \frac{0.5(R_{f1} + R_{f2})}{R_g}$. What does change however, is that a purely differential input has the differential output with an amplification of A_{V0} combined with some common-mode output. For example, if X_2's feedback resistor is replaced by a short and X_1's is equal to R_f and a symmetrical DC input signal of ±ΔV is applied on both inputs, then the output of X_2 goes down by ΔV while the output of X_1 goes up by $(1 + 2R_f/R_g)\Delta V$. That is the correct differential output but there is also a common-mode of offset of $(Rf/Rg)\Delta V$. This is only the case as described above, for reasonably matched feedback resistors there is no problem [18].

The second stage of the instrumentation amplifier consists of one difference amplifier, also called the subtractor. This stage is a unity gain differential amplifier, which has an output where the output is the difference between the two inputs. There will be a unity gain for the differential signal while removing the common-mode signal. For this reason, the resistors of the difference amplifier are equal.

In total, the gain of the instrumentation amplifier will be equal to the gain acquired in the first stage, so that is $A_{instrumentation} = (1 + R_f/R_g)$. Normally, the gain of the circuit can now also be changed by replacing only the two gain resistors, R_g, while not changing the symmetry of the circuit.

2.1.2 AC-coupling network

The biopotential signals which the electrodes will acquire are alternating current (AC) signals superimposed on relatively large DC voltages. An ac-coupling network removes this DC voltage offset while letting the AC signal pass. One of the simplest techniques for a differential amplifier, shown in figure 5 (a), is a passive differential high-pass filter in front of a DC-amplifier. The grounding resistor R_2 of this network reduces the input common mode impedance which effects the CMRR negatively due to the potential divider effect [15].

Different differential ac-coupling networks are compared in the study of Casas et al. The networks are based on first order, high-pass filters in front of an instrumentation amplifier. The focus in this study is on having a network with a high CMRR to avoid compromising the CMRR of the entire analog processing circuit chain. Another requirement of the network is that it does not use separate grounded components per signal line [19].

The study shows that the network in figure 5 (b) has the highest CMRR for frequencies from 0.1 – 10 Hz and a CMRR equal to the other networks for higher frequencies. The transient response of this circuit was also good compared to the other networks, as shown in figure 6. The chosen ac-coupling network consists of two single-ended, high-pass filters whose common node is connected to the input common-mode voltage obtained by an ungrounded passive voltage adder.

The formula of the differential gain is given by formula 5, where $\tau_1 = R_1 C$, $\tau_1' = \mathrm{R}_1' C'$, $\tau_2 = R_2 C$, $\tau_2' = \mathrm{R}_2' C'$. A simplification is possible if $\tau_2 = \tau_2'$ which results in:

$$G_{DD}(s) = \frac{\tau_1 \mathrm{s}\,[1 + (\tau_1 + \tau_2)\mathrm{s}]}{(1 + \tau_2 \mathrm{s})\,[1 + (\tau_1 + \tau_2)\mathrm{s}]} = \frac{\tau_2 s}{1 + \tau_2 s} \qquad (5)$$

After the simplification of the formula, it shows the formula of a first-order, high-pass filter. The gain is only dependent on R_2 and C. To show this, the calculations of the CMRR of the AC-coupling system are simplified, $R_1 = R_2 = R$ and $\tau_2 = \tau$, resulting in formula 6.

$$CMRR(s) \approx \frac{C}{C_{in}} x \frac{1 + 2\tau s}{\Delta R/R + \Delta C_{in}/C_{in} + 2\tau(\Delta C/C + \Delta C_{in}/C_{in})s} \quad (6)$$

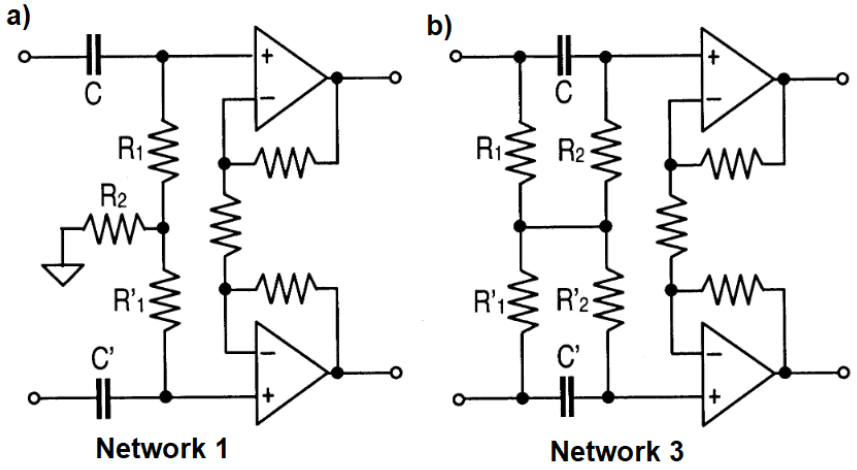

Figure 5: AC coupled networks. a) passive differential high pass filter in front of a DC-amplifier b) Fully differential passive AC-coupling network built by mirroring two single-ended, high-pass filters whose common node is connected to the common-mode input voltage obtained through an ungrounded passive voltage adder [15, p. 391]

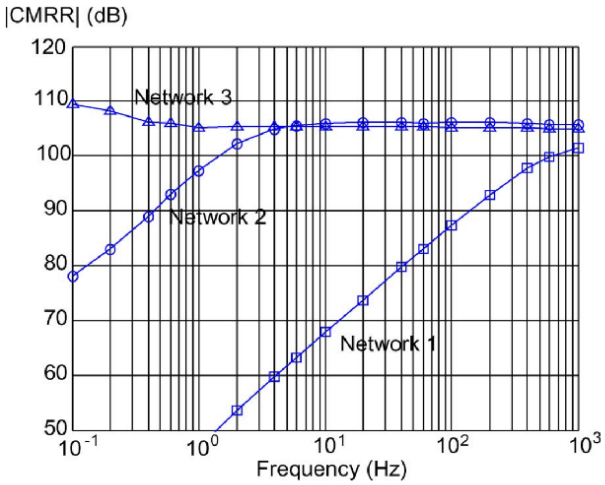

Figure 6: Graph displaying CMRR (dB) on y-axis in function of frequency (Hz) on x-axis. Used network (network 3) compared with the other networks [19, p. 97]

2.2 DC restoration

The ac-coupling network removes the DC input voltages. However, offset voltages can be generated in the previous stages. This includes the op amp input offset voltage, where the offset is amplified as input signals. With a gain of 1000, the difference in input offset voltage of 1 mV will result in 1 V at the amplifier output. Not only that, but the op amps input voltage noise and the thermal noise of R_2 and R_2' from dc to the frequency $f_{c,2} = 1/2\pi R_2 C$ are amplified. To solve this problem, a DC restoring circuit, as shown in figure 7, is added to remove the offset voltages and reduce 1/f noise by rejecting low frequencies. This DC restoration ensures a DC baseline level to fully exploit the input range of the ADC while also blocking low frequency noise [15], [20], [21].

To achieve this, an integrator is placed in a feedback loop around the last difference op amp of the instrumentation amplifier. This integrator will work as a first order high-pass filter with the transfer function given by formula 7, where $\tau_i = R_i C_i$ and $A_i = R_6/R_5$. As said in section 2.1.1, resistors $R_5 = R_5' = R_6 = R_6'$ which results in $A_i = 1$ because the last differential amplifier is a unity gain. The cut-off frequency of this filter can be found at $f_{c,i} = 1/2\pi R_i C_i$.

$$T_i(s) = \frac{\tau_i s\, A_i}{1 + \tau_i s} \tag{7}$$

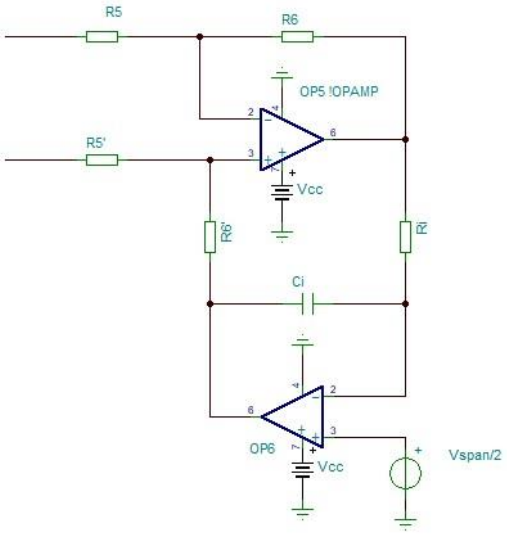

Figure 7: DC restoration circuit, an integrator in feedback loop around difference amplifier

2.3 Driven Right Leg

As explained in section 1.2, powerline interference, together with other common-mode interference, is noise that is present in any biopotential measurement and can disturb relevant signal features. One technique to try to remove this noise is the Driven Right Leg (DRL) technique. This technique senses the unwanted common mode potential, inverts it and then compares it with a DC voltage or ground. The difference is then injected back into the patient, reducing the common mode potential. It traditionally got the name because the electrode is attached to the patient his right leg, which is the furthest away from the heart [22].

The driven right leg used in this paper compares the common mode potential with a DC voltage, driving the patient's potential to a known DC offset which allows the circuit to be operated by a single supply. The DC voltage is commonly chosen to be $V_{cc}/2$.

The current limiting resistor R_0 ensures the patient's safety in case of a potential short circuit. It limits the current during this possible short circuit which would lead to a saturated op amp. V_{short} in this formula is typically V_{cc} that powers the op amp. For a system with V_{cc} = 5 V, the minimum resistance is 100 kΩ. For a power supply of 3 V, a minimum of 60 kΩ is required [23]. The current that flows through the patient should be limited, as this is the factor that damages the body.

2.4 Low pass filter

The previous stages block the unwanted common-mode voltage and the low frequency signals while amplifying the differential signals. The last stage of the circuit only focuses on removing the high frequency noise.

To block high-frequency noise, a low-pass filter is added in the last stage. More specifically a Sallen-Key low-pass filter [24]. This is a second-order filter with two poles. The first step to design this filter is to choose the cut-off frequency f_c.

The cut-off frequency can be calculated by using formula 8. The formula can be simplified by taking $R_1 = R_2 = R$ and $C_1 = C_2 = C$.

$$f_c = \frac{1}{2\pi\sqrt{R_1 C_1 R_2 C_2}} = \frac{1}{2\pi RC} \tag{8}$$

The transfer function of this filter is given by formula 9. The gain of this stage for each frequency can be calculated using formula 10.

$$T(s) = \frac{V_{out}(s)}{V_{in}(s)} = \frac{(2\pi f_c)^2}{s^2 + 2\zeta(2\pi f_c)s + (2\pi f_c)^2} = \frac{{\omega_n}^2}{s^2 + 2\zeta\omega_n s + {\omega_n}^2} \tag{9}$$

$$M(\omega) = |G(j\omega)| = \frac{{\omega_n}^2}{\sqrt{({\omega_n}^2 - \omega^2)^2 + 2\zeta(\omega_n\omega)^2}}, (\omega = 2\pi f) \tag{10}$$

Where ζ is the damping ratio of the system and Q = 1/2ζ. In this system Q = 0.5 is desired which also means $\zeta = 1$, also called a critically damped system. In other words, the system will return to its equilibrium as soon as possible after each change, without oscillation and without overshoot. Another result is that the system has a double pole $p_1 = p_2 = -\omega_n$. Also, the gain at the cut-off frequency f_c of a second-order filter is -6 dB with a decay of -40 dB/decade, as shown in figure 8 [25].

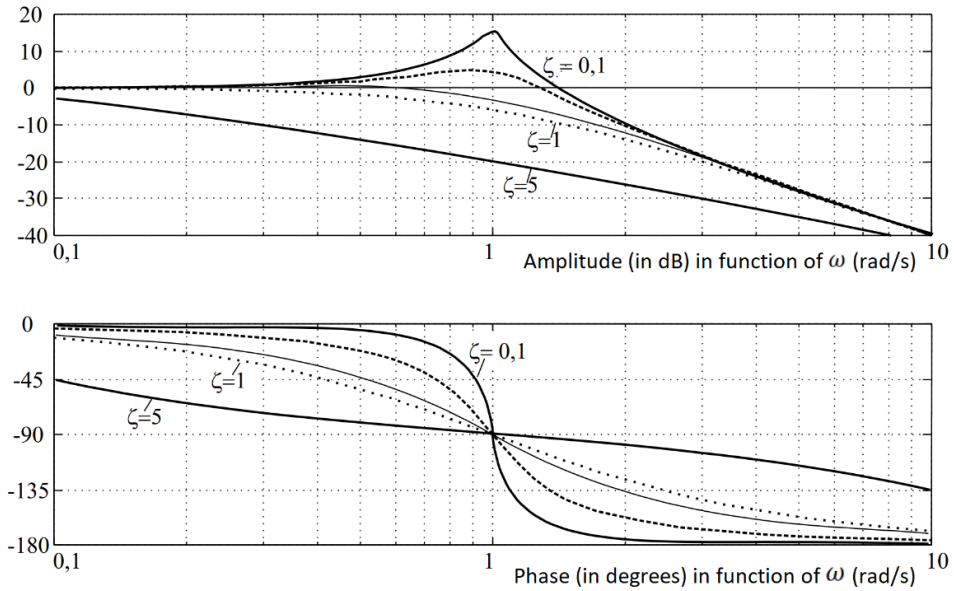

Figure 8: Bode-diagram of second order system with different damping coefficients and cut-off frequency (w_n = 1, K =1) [25, p. 44]

3 Materials

In this chapter of the thesis, an overview is provided on the selection of materials employed in the fabrication of a bio amplifier for each of the provided electrograms. The calculations required to determine the optimal values of the components and the formula for obtaining the expected frequency response are also presented. Each stage of the bio amplifier is verified through individual simulations using Tina TI, a SPICE-based analog simulation program developed by Texas Instruments.

The gain or the attenuation of signals below are expressed in decibel (dB). This makes it easier to compare gain and attenuation of signals as well as easy comparison with the frequency response simulations. The formula to configure the gain to decibels can be found in formula 11.

$$G_{dB} = 20 * log_{10}(Gain) \quad (11)$$

3.1 Requirements

The goal of this amplifier is to introduce students to work with a more accurate amplifier board than with, for example, a breadboard build amplifier. On some occasions, the decision has been made to work with more standard values instead of exactly calculated values. The reason for this is that one criteria of the board is to minimize costs, while being able to perform the electrograms. This is also the case for the tolerances of the resistors and capacitors. It is desired that this device can be powered by a single supply, e.g., by one battery.

A second criterion of this design is that it has to fit on a 2-layer Printed Circuit Board (PCB) of 50 x 100 mm. Later, two designs can be joined on a single PCB of 100 x 100 mm. The main reason for this requirement is the cost: the supplier of the PCB charges the same amount for 10 pieces of 50 x 100 mm as for 10 pieces of 100 x 100 mm.

Another criterion is that all components have to be through-hole components, such as Dual In-line Package (DIP) instead of the smaller and more stable Surface-Mount Devices. This has a simple explanation; students need to be able to solder the components themselves onto the PCB and DIP is much easier to do without destroying components. Furthermore, it is easier to probe and troubleshoot larger components.

3.2 Bio simulator

The in-house developed bio simulator is a programmed waveform generator that utilizes a DAC (digital-to-analog converter). It generates different ECG signal waveforms based on the user input from two buttons. The first button can select different waveforms, the second button inverts the waveform. Lastly, there is a potentiometer to adjust the frequency of the signal.

The device continuously loops, updating the ECG waveform based on the selected configuration and controlling the duration and characteristics of the signal. There are two output pins and one reference pin. There is one output pin called V+, which has the highest potential waveform and V-, which has a slightly smaller positive output signal. The reference pin is available to give feedback to the device. In summary, this device provides a versatile solution for generating simulated ECG signals.

The three pins on the right of figure 9 are the output and reference pins, where the reference pin is in the middle. It is possible to power this board with a 5 V or 9 V DC power supply. The light emitting

diode next to the +5 V pin emits light when the board is powered on. The red LED blinks on the frequency of the heart signal.

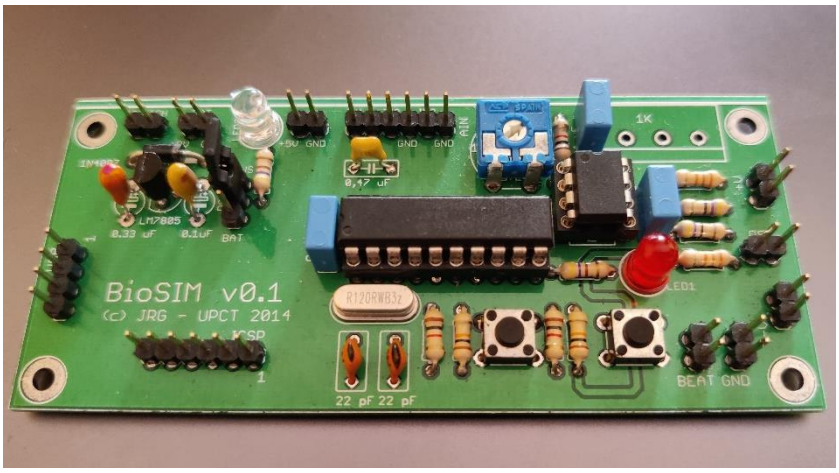

Figure 9: Bio simulator that generates an ECG signal

3.3 Electrodes

The usage of electrodes is necessary to collect the potential differences on the body. An electrode is the place where the shift from electronic to ionic conduction takes place. The electrolyte gel is the ionic part, and the metallic part is the electronic part. The contact medium between the metallic part of the electrode and the tissue is an ionic conductor by definition. The contact medium is important for having minimal noise on the signal as well as a low source impedance [26].

For that reason the chosen electrodes are the Swaromed general monitoring electrodes from Nissha Medical Technologies [27]. These electrodes are for single use and pre-gelled. The electrode uses wet gel with a foam sponge and Ag – AgCl sensor polymer which functions as a reversible redox electrode. It can be used for 48 hours when applied and it has a shell-life of 36 months when the electrode stays in its package. The ACZ impedance at 10 Hz is below 300 Ω, and the ACZ impedance repeat is below 150 Ω.

The electrodes are connected to the medical electrode adapter cable, displayed in figure 10. This cable has a 3.5 mm male jack output and three different color-coded connectors to the electrodes. The yellow electrode corresponds to the front tip of the 3.5 mm jack, the green cable to the middle part and the red cable to the back part.

Figure 10: Medical electrode adapter to 3.5 mm jack [28]

3.4 Output of the amplifier

For safety reasons, the output of the biopotential amplifier cannot be connected to a regular, not isolated oscilloscope. For this reason, the faculty of biomedical engineering of the Polytechnic University of Cartagena use Biopac Systems Inc. to teach their students how to work with medical devices.

The data acquisition system used to read out the biopotential amplifier of this work, is the Biopac MP35 [29]. The device has an internal microprocessor that makes it possible to communicate with a computer by a USB connection while also controlling the data acquisition. At the front side, it has four 9-pin female channels that work as the input as shown in figure 11. The device receives the signal by a differential input, thus through two pins, V_{in}+ and V_{in}-, which are internally subtracted to obtain the signal. Although the device receives the output of the PCB, it also works as a supply source with pins for +5 V and -5 V DC voltage. Another pin is reserved for the ground. A DB9 cable is used to connect to the channels.

The MP35 has passed the Medical Safety Test Standards IEC 60601-1 as well as the Medical Electromagnetic Compatibility (EMC) Test Standards. The analog input voltage range is adjustable from 200 µV to 2 V. It has a fixed hardware low pass filter at 20 kHz and a fixed hardware high pass filter of minimum 0.05 Hz [30].

The MP35 can be connected to a computer by a USB A cable. Extra precautions are added by placing an additional USB port isolator between the computer and the MP35 output. The used isolator is the ADuM31601 from Analog Devices, which has upstream short circuit protection and bidirectional communication [31]. The device is connected to the computer that uses the software to view the output of the MP35. It is recommended that the used computer is a laptop which is disconnected from the electrical grid.

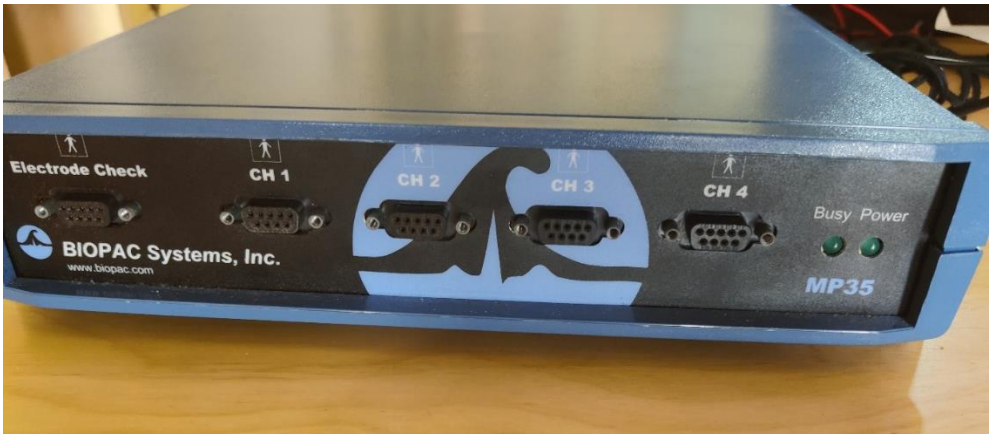

Figure 11: Biopac MP35. A data acquisition system with four channels

The software responsible for controlling the MP35 and processing the data on the laptop is Biopac Student Lab, BSL 7.0 Pro. A channel can be selected as the input to display on a graph. Then an amplification between 10 and 500 can be selected, while also applying additional digital filters to the received signal. Three different filters can be applied on one input channel, like a low or high pass and band stop or band pass filter from a selected frequency.

To explore lower cost alternatives to the Biopac MP35 paired with its additional software, the output is also tested on the analog-in pin of an Arduino Uno. The Arduino Uno is a common development board which has multiple applications, but one of the features it has is reading analog signals through one of its analog pins. The signal goes through a built-in analog to digital conversion, which has a 10-bit resolution or 1024 levels resulting in a theoretical accuracy of 4.88 millivolts. Thus, a digital output of '1' from the Arduino Uno is actually 4.88 mV. It is possible to use the on-board serial communication to hand the data off the host computer. The Arduino Uno board is powered with 7 V – 12 V power supply or via an USB 5V of a computer [32].

3.5 Simulation software

All simulations are executed on TINA-TI [33]. Texas Instruments has developed a SPICE-based analog simulation program. To begin using this program, the initial step involves creating an electrical circuit. Within the program, it is possible to select an ideal component with a specific value or configure its parameters. For instance, when working with a resistor, parameters such as power rating, temperature limits, and linear temperature coefficient can be adjusted to meet specific requirements. Additionally, various types of power sources and meters can be added to the circuit.

Once the circuit is created, it can be simulated using the program. The simulation process involves utilizing tools such as the multimeter or oscilloscope, which can be utilized throughout the entire circuit. Furthermore, the program offers different types of analyses, including AC, DC and transient analysis of the circuit. The AC frequency response is used to simulate the different stages as well as whole circuits. This AC frequency response analysis facilitates the understanding of how circuit's performance varies across different frequencies.

3.6 Electrical characteristics of circuit based on signal

In section 1.1, the function of each type of measurement is explained. In this section, the focus will be on the electrical characteristics. Table 1 displays the desired upper and lower bandwidth frequencies of each of the signals as well as their expected amplitudes. The circuit needs to make a band-pass filter based on the bandwidth of the signals while also amplifying the signal with a predefined gain.

The lower bandwidth 0.05 Hz is the exact lower frequency for a normal ECG. This frequency is also chosen for EEG, where the optimal is 0.5 Hz and for EOG, where the optimal is little below 1 Hz. In the case of EOG, it looks like this is too big of a difference, but the EOG signal frequency starts at 0 Hz while 90% of the signals can be found between 1 and 12 Hz, thus 0.05 Hz is a good cut-off frequency. As later seen in the design of the PCB, it is helpful to have only two different lower cut-off frequency options for all signals.

The chosen upper cut-off frequency of each signal is more specific. The chosen bandwidth for the ECG measurement has the typical bandwidth of 0.05 – 150 Hz. The total bandwidth of the Electromyography is chosen to be between 20 and 500 Hz. The reason for this is because the sources have various opinions on the necessary upper cut-off frequency, where [5] states that the bandwidth should be 6 Hz to 600 Hz and [6] states it is between 15 Hz and 400 Hz. The chosen upper limit is the average of the two while the lower limit is set at what [5] says to be the lower limit of the dominant frequency bandwidth, namely 20 Hz. The upper limit of EEG is set at 40 Hz because the frequency of the signal is until 100 Hz, where the most interesting signals can be found below 30 Hz. The band limit of the EOG signals is from 0 to 50 Hz. Almost 90% of the EOG signal can be found between 1 and 12 Hz. That is why the upper limit of 10 Hz is chosen.

Table 1: Electrical characteristics of ECG, EMG, EEG and EOG. Upper and lower frequency (in Hz) and the amplitude (in µV)

Electrical characteristic of different type of signals			
	Bandwidth		
Signals	Lower (Hz)	Upper (Hz)	Amplitude (µV)
Electrocardiogram (ECG)	0.05	150	10 – 2000
Electromyography (EMG)	20	500	10 – 5000
Electroencephalogram (EEG)	0.05	40	10 - 300
electrooculogram (EOG)	0.05	10	50 - 3500

Beside the band limiting of the received potential, the task of the biopotential amplifier is to amplify the difference signal. A typical gain of 1000, or 60 dB, is used for an ECG amplifier. This gain is also sufficient for EMG and EOG. For EEG a gain of 2000, or 66 dB, is necessary because of the low amplitude of around 300 µV. These gains are chosen so that the peak of the signal stays between ground and the selected V_{cc}.

The designed bio amplifier is first tested on a bio simulator. This device is connected to a power supply and it produces an artificial heart beat signal with a peak-to-peak amplitude of around 7000 µV. The gain of the biopotential amplifier is lowered to a gain of 92 when testing, to not saturate the op amps.

3.7 Overview of total circuit

The designed biopotential amplifier has an instrumentation amplifier at its core with additional circuitry added to satisfy the requirements. The circuit is split into different stages to be able to simulate the frequency response of each stage separately with different component values. An overview of the proposed circuit is illustrated in figure 12.

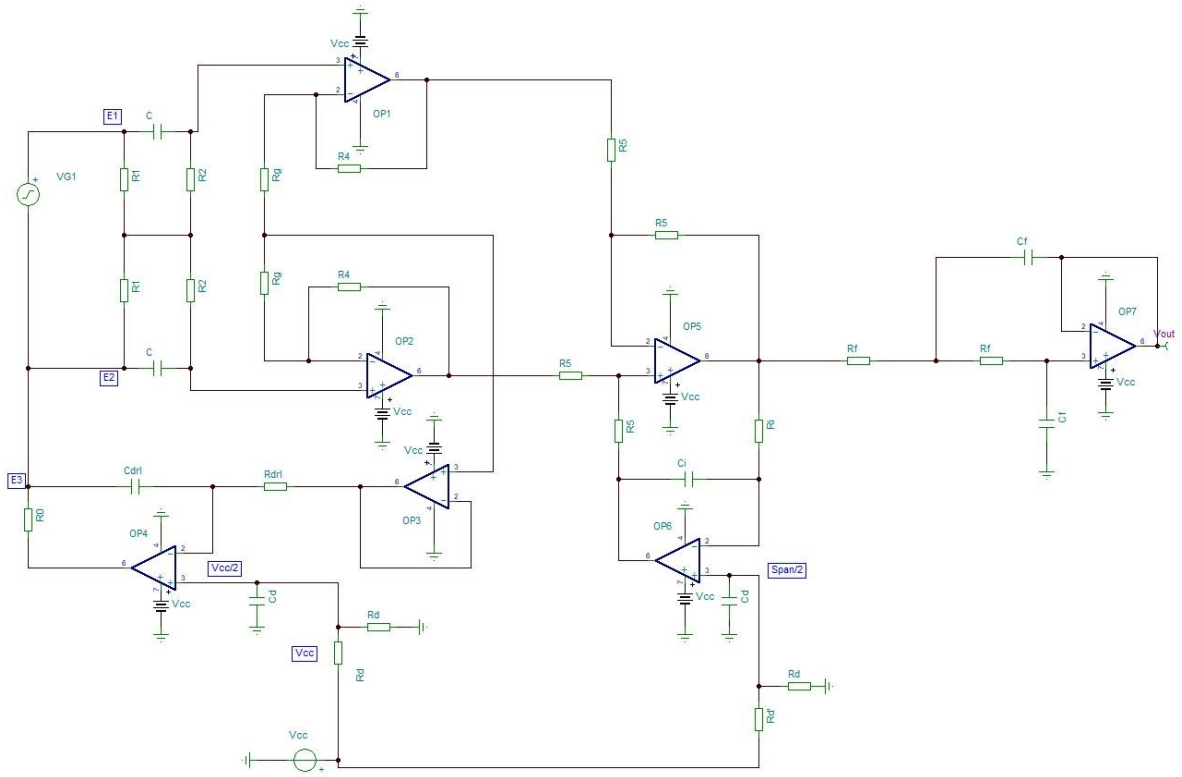

Figure 12: Overview of the proposed circuit for the bio amplifier

3.8 AC-coupling network

The AC-coupling network's first task is to remove the DC voltage and let the differential signal pass, thus having a high CMRR. Another requirement is that this stage has a very high input impedance compared to the electrode-skin contact. According to [15], the input impedance of an electrocardiogram should be higher than 2.5 MΩ, thus a value for R_1 = R_2 = R = 4.7 MΩ fulfills this requirement. With $\tau_2 = R_2C$, $\tau_2' = R_2'C'$, the transfer function of this system is equal to that of a first-order, high pass filter or formula 5. The gain is only dependent on R_2 and C.

The cut-off frequency for a first-order high pass filter can be found for $f_c = 1/(2\pi R_2 C)$. The formula is converted to calculate the capacitance C, because the desired cut-off frequency f_c = 0.05 Hz. This results in

$$C = \frac{1}{2\pi R_2 f_c} = \frac{1}{2\pi * 4.7 * 10^6 \Omega * 0.05\ Hz} = 0.677 * 10^{-6} F$$

There is a common value of 0,68 µF but an even more normalized value of capacitors is 1 µF. With C = 1 µF and R = 4.7 MΩ, $\tau_2 = R_2C = 4.7$ The gain of this stage can be calculated by converting formula 5 to the gain in function of ω (rad/s) where ω = 2π*f.

$$M(\omega) = |T(j\omega)| = \frac{\tau_2\omega}{\sqrt{1+{\tau_2}^2\,\omega^2}} = \frac{4.7\omega}{\sqrt{1+4.7^2\,\omega^2}} \tag{12}$$

The gain can now be calculated for each frequency, for example:

$$M(\omega)_{dB} = 20 * log_{10}\left(\frac{4.7 * (2\pi * 0.05)}{\sqrt{1+4.7^2\,(2\pi * 0.05)^2}}\right) = -1.64\ dB$$

This is lower than the desired cut-off frequency. The new cu-toff frequency can be found at

$$f_c = \frac{1}{2\pi * 4.7 * 10^6\Omega * 10^{-6}F} = 0.0338\ Hz$$

In figure 13, the circuit is implemented in TINA-TI where the voltage source is ideal, with no impedance and the result of the frequency response is shown. The frequency response shows that this is a high pass filter with a cut-off frequency at 0.034 Hz followed by a -20 dB decay per decade.

Figure 14 displays the output voltage in function of a changing source resistance. When only a common mode voltage is applied to this circuit, the difference at the output voltage equals zero. This shows that the AC-coupling stage blocks common mode voltage.

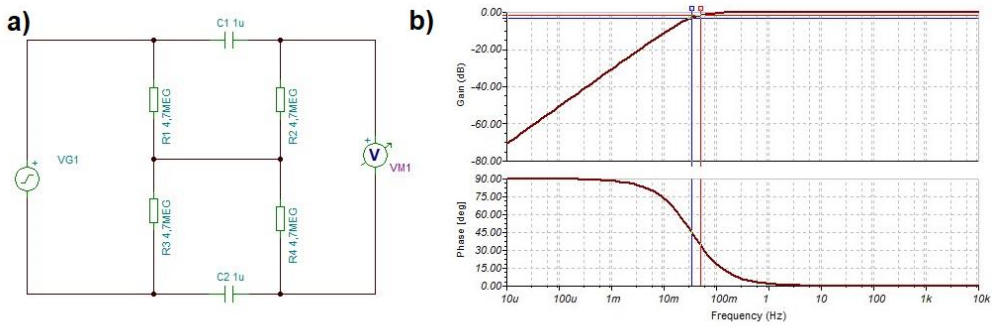

Figure 13: a) AC-coupling circuit with no source impedance b) AC transfer characteristics frequency response simulation with the gain on the y-axis in dB and the frequency on the x-axis in Hz. The red line is at 0.05 Hz and -1.65 dB. Blue line is on 0.034 Hz and -3 dB

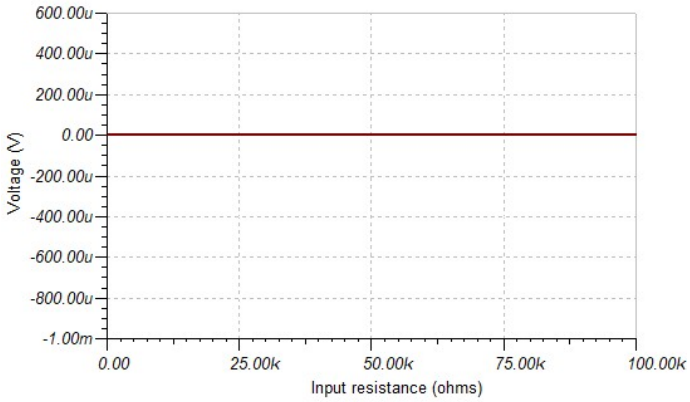

Figure 14: DC transfer characteristics where the output voltage (in V) on the y-axis is in function of source resistance (in Ω) on the x-axis

3.9 Instrumentation amplifier

The ac-coupling stage is followed by the instrumentation amplifier. The first stage of the instrumentation amplifier determines the gain of the amplifier and has a differential output. The gain resistor is divided into two resistors because the driven right leg will be connected in between to inject the common mode voltage back to the patient.

The total gain of the instrumentation amplifier is calculated using the formula 13:

$$G_{instrumentation} = 1 + \frac{R_f}{R_g} \tag{13}$$

For the Electrocardiogram, electromyography and electrooculogram a gain of 60 dB or 1000 is desired. To make calculations and component selection easier, the aimed gain is 1001 so R_f/R_g = 1000. For example, the peak-to-peak amplitude of an ECG signal is 1 mV and with a gain of 1000 this would result in a peak-to-peak amplitude of 1 V. The gain for Electroencephalogram should be 66 dB or 2000. This configuration and its respective AC frequency response is illustrated in figure 15.

The gain resistor for an amplification of 2001 is set to be R_g = 100 Ω. The next step is to determine R_f by converting formula 13 to R_f. As a result, R_f = 200 kΩ. If the gain is set lower, to 60 dB, R_g should be changed. If R_f stays constant, R_g = 200 Ω.

For testing however, the bio simulator produces an artificial heartbeat with a peak-to-peak amplitude of 7000 µV. If an amplification of 60 dB or 1001 would be applied to this signal, an output signal of 7 V would be the result. This would saturate the op amp, which has a supply voltage of 5V. For this reason, the desired gain is 100 or in other words R_g = 2 kΩ. In the prototype device, R_g of 2.2 kΩ had to be used because 2 kΩ was unavailable. This modification results in a gain of 92.

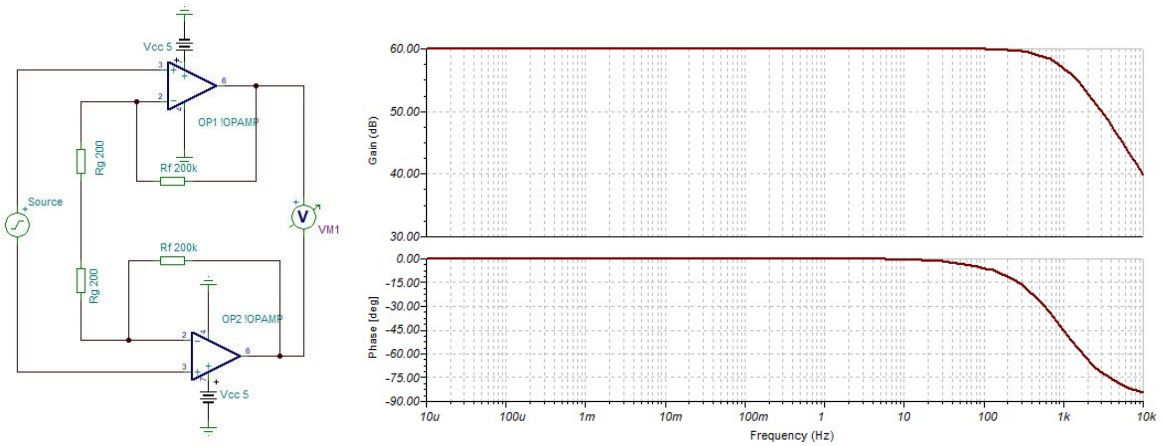

Figure 15: Stage 1 of the instrumentation amplifier, gain is set at 1001. On the right is the ac frequency response of the circuit with the gain (dB) on the y-axis and the frequency (Hz) on the x-axis

3.10 DC restoration

The DC restoration circuit is an integrator placed in a feedback loop around the difference amplifier as shown on the left image of figure 16. As stated previously in section 2.1.1, the resistors of the difference amplifier are equal, resulting in a unity gain amplifier. The integrator works as a high pass filter while also creating a DC offset voltage at the output.

The cut-off frequency of the DC restoration circuit can be found at $f_c = 1/(2\pi*R_i*C_i)$. For $R_i = 10$ MΩ and $C_i = 1$ µF, the cut-off frequency is $f_c = 0.016$ Hz. The transfer function of the circuit in figure 16 is given by formula 7. With formula 14, where the gain is in function of the angular frequency ω, the previous calculated cut-off frequency can be verified. As expected, the result of $M(2\pi*0.016) = -2.99$ dB. When the formula is used for the desired cut-off frequency of 0.05 Hz, $M(2\pi*0.05) = -0.42$ dB. These calculations are supported by the simulations shown on the right image of figure 16. The simulated gain for f = 0.05 Hz is 0.49 dB and the cut-off frequency at -3 dB is found at 0.0164 Hz.

$$T_i(s) = \frac{\tau_i s\, A_i}{1 + \tau_i s} \tag{7}$$

$$M(\omega) = \frac{\tau_i \omega}{\sqrt{(1 + \tau_i{}^2 \omega^2)}} \tag{14}$$

$$M(2\pi * 0.05) = 20 * \log\left(\frac{10 * (2\pi * 0.05\,)}{\sqrt{(1 + 10^2 (2\pi * 0.05)^2)}}\right) = -0.42\ dB$$

The low cut-off frequency of an electromyography (EMG) is set at 20 Hz. The resistance of R_i is changed to be able to achieve a narrower bandwidth. When using the $f_c = 1/(2\pi*R_i*C_i)$ where $C_i = 1$ µF and $f_c = 20$ Hz, the ideal $R_i = 7.96$ kΩ. This is not a standard value, and the closest available value was $R_i = 10$ kΩ which results in a $f_c = 16$ Hz. The theoretical gain can be calculated using formula 14, with an updated $\tau_i = 0.01$. The result of $M(2\pi*20) = -2.13$ dB.

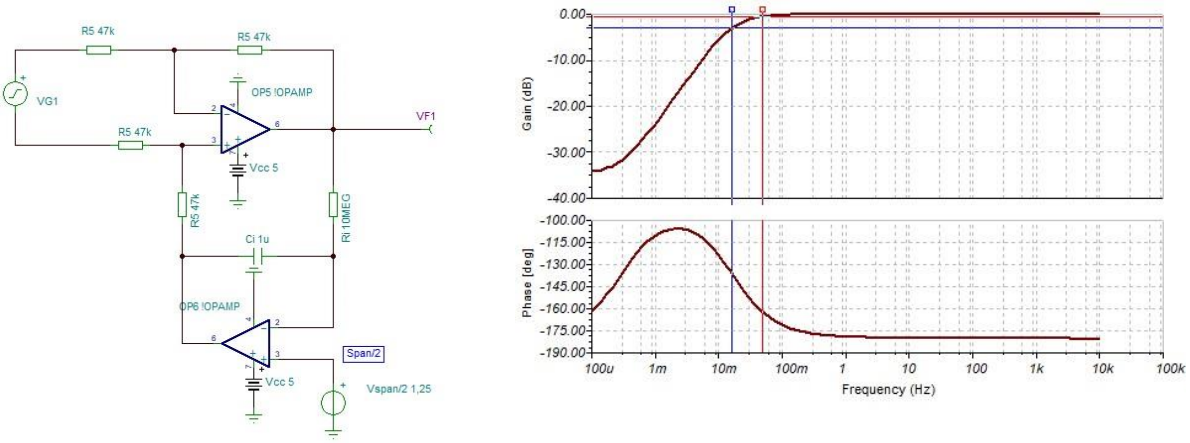

Figure 16: On the left the circuit of an integrator in a feedback loop around the difference amplifier. On the right the AC frequency response of this circuit with the gain (dB) on the y-axis and the frequency (Hz) on the x-axis. The red line is set at 0.05 Hz with an amplitude of -0.49 dB. The blue line is set at the cut-off frequency, -3 dB, at 0.0164 Hz

The DC offset is created by applying a DC voltage at the non-inverting input of the op amp. This DC offset at the output will be equal to the applied voltage on this port. The bio amplifier will be powered by one battery, thus the DC voltage chosen will be lower than that of the battery. Another point to keep in mind, the amplified differential signal plus this DC offset needs to stay below the battery voltage.

The signal of about 1 mV amplified results in a signal of about 1 V. In the case of the bio simulator, the signal is 6 mV, but the output signal will be around 600 mV when amplified with a gain of 101. A rather safe approach is to take a DC offset of one-fourth of the battery supply V_{cc}. A voltage splitter is created to achieve this division. Using $V_{out} = \frac{R_2}{R_1+R_2} * V_{in}$ where V_{out} is the chosen DC offset and V_{in} is our battery voltage or V_{cc}. The result is that $\frac{R_2}{R_1+R_2} = \frac{1}{4}$. The chosen values are R_1 = 200 kΩ and R_2 = 68 kΩ. It is possible to change this DC offset later by replacing R_2 for a different resistance.

The required cut-off frequency for ECG, EOG and EEG, as displayed in table 1, is 0.05 Hz. If the gain is calculated for 0.05 Hz, the value of -0.42 dB does not achieve the required attenuation of -3 dB. However, the previous stages influence the final output response of this stage as well. The combination of these stages is shown in the left image of figure 17. The result of the combination of the transfer functions is given by formula 15, where A_{V0} is the gain of the instrumentation amplifier and τ_2 is the time constant of the AC-coupling network.

$$T(s) = \frac{\tau_2 s}{1+\tau_2 s} \cdot \frac{\tau_i s \cdot A_{V0}}{1+\tau_i s} \tag{15}$$

$$M(\omega) = \frac{-A_{V0}\tau_2\tau_i\omega^2}{\sqrt{(1+{\tau_2}^2\omega^2)*(1+{\tau_i}^2\omega^2)}} \tag{16}$$

$$M(2\pi * 0.05) = 20 * log_{10}\left(\frac{1001 * 4.7 * 10 * (2\pi * 0.05)^2}{\sqrt{(1+4.7^2*(2\pi*0.05)^2)*(1+10^2*(2\pi*0.05)^2)}}\right) = 57.95\ dB$$

The total gain is calculated using formula 16, on the required 0.05 Hz. The gain in the previous stage A_{v0} is set at 1001 for this calculation of an ECG amplifier. This results in a gain of about 60 dB for the

desired frequencies between 0.05 Hz and 150 Hz. The gain at the cut-off frequency should be $M(2\pi*f_c)$ = $Gain_{max}$ – 3 dB. The calculated gain at 0.05 Hz is 57.95 dB and the simulated gain, shown on the right of figure 17, is 57.79 dB. Thus, the cut-off frequency is lower. When the formula is transformed to calculate the frequency at a gain of 57 dB, the result is 0.04 Hz which is equal to the simulated frequency.

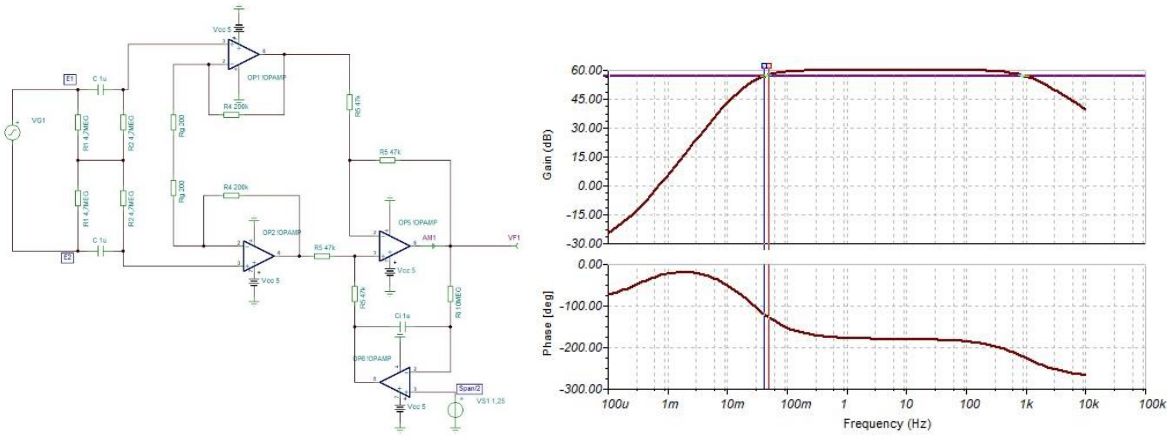

Figure 17: Left: The DC restoration circuit combined with the AC-coupling network and the instrumentation amplifier. On the right the AC frequency response for A_{v0} = 1001 and R_i = 10 MΩ with the gain (dB) on the y-axis and the frequency (Hz) on the x-axis. The red line at 0.05 Hz has a gain of 57.79 dB. The blue line has a gain of 57 dB at 0.04 Hz

3.11 Driven Right Leg

The driven right leg circuit drives the potential of the patient to a known DC offset. The R_{drl} as displayed in figure 18 should be a low value resistance. This common-mode resistor provides a low-impedance path for the common-mode noise. With [15], [34] as examples, the chosen value of R_{drl} = 10 kΩ.

The known DC offset is set at $V_{cc}/2$. This is to make sure that the signal at the electrodes E1 and E2 are between 0 V and V_{cc}, allowing a single supply operation. The V_{cc} divided by two is acquired in the same way as $V_{cc}/4$ as in the DC restoration circuit, namely a voltage splitter. To divide the voltage by two, two equal resistors are chosen. $R_1 = R_2 = R$ = 200 kΩ.

The capacitor between the inverting input of the op amp and the right leg electrode makes the feedback loop an open circuit when a DC voltage is supplied but passing higher frequency signals. There will be an offset DC voltage at the output, which should not be returned to the inverting input of the op amp. This capacitor is set at 10 nF resulting in a frequency response, shown in figure 19.

The safety of the patient needs to be ensured at all times. That is why a protection resistor R_0 is added behind the last driven right leg op amp. In case of a short in the circuit, the maximum output of the op amp will be the power supply. In this case, the power supply will be 5V. The required resistance is at least 100 kΩ according to [23], but to calculate the output current that will be driven to the patient the following formula is used.

$$i_{short} = \frac{V_{short}}{R_0} \tag{17}$$

The work that formed the base of the proposed biopotential amplifier uses a protection resistor of R_0 = 510 kΩ to drive the current to around 10 µA. For a V_{short} of 5V this would result in i_{short} = 9.80 µA when using the formula. This current is considered safe to the patient in case of an amplifier fault.

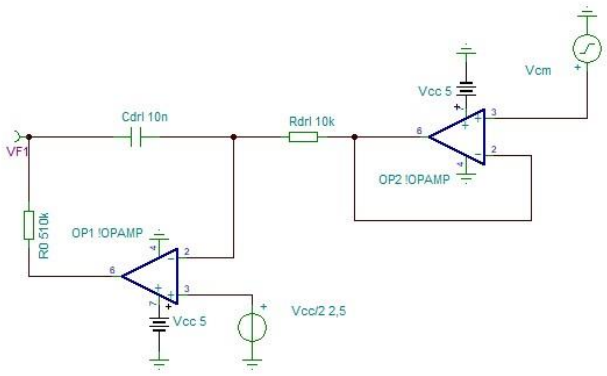

Figure 18: Used driven right leg circuit

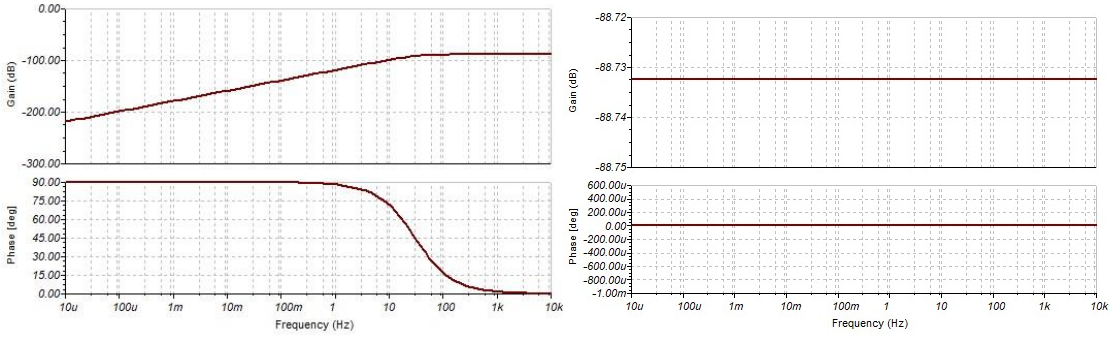

Figure 19: Left: AC frequency response of driven right leg circuit with a C_{drl} of 10 nF. Right: The AC frequency response of the driven right leg circuit with no C_{drl}. For both graphs the gain (dB) on the y-axis and the frequency (Hz) on the x-axis

3.12 Low pass filter

A second order Sallen Key Low pass filter is used to block the unwanted high frequency signals. The transfer function, given by formula 19, displays that this filter is a second order low pass with two poles on -ω_n. The damping ratio of this filter is set at $\zeta = 1$.

$$f_c = \frac{1}{2\pi R_f C_f} \tag{18}$$

$$T(s) = \frac{V_{out}(s)}{V_{in}(s)} = \frac{(2\pi f_c)^2}{s^2 + 2\zeta(2\pi f_c)s + (2\pi f_c)^2} = \frac{{\omega_n}^2}{s^2 + 2\zeta\omega_n s + {\omega_n}^2} \tag{19}$$

$$M(\omega) = \frac{(2\pi f_c)^2}{\sqrt{-\omega^4 + 4 * 1 * (2\pi f_c)^2 * \omega^2 + (2\pi f_c)^4}} \tag{20}$$

Each electrogram requires a different upper cut-off frequency. In this study, the ECG requires a cut-off frequency at 150 Hz. Following the formula, f_c set at 150 Hz would result in $2\pi f_c = \frac{1}{R_f C_f} \rightarrow R_f C_f = 1.06 * 10^{-3}$. There is a preference for more standardized values for the

capacitor and the resistor. So, when the values are set at R_f = 100 kΩ and C_f = 10 nF, the cut-off frequency f_c = 159 Hz. Figure 20 shows the simulation of this stage for these values. The attenuation at 159 Hz is 6 dB, because the Sallen Key Low pass filter is a second order filter. This is followed by an attenuation slope of -40 dB per decade. When using formula 20, for a frequency of 150 Hz, or ω = 2π*150, the attenuation results in -5.76 dB. This is supported by the simulation where an attenuation of -5.56 dB is expected at 150 Hz.

The capacitors are kept constant for the other cardiograms. In this way, only the resistors need to be configured to change the cut-off frequency of this low pass filter. Formula 18, is used to calculate the required resistance to achieve the cut-off frequency. Then the resistance value closest to the calculated value is chosen. The used resistors are displayed in table 2.

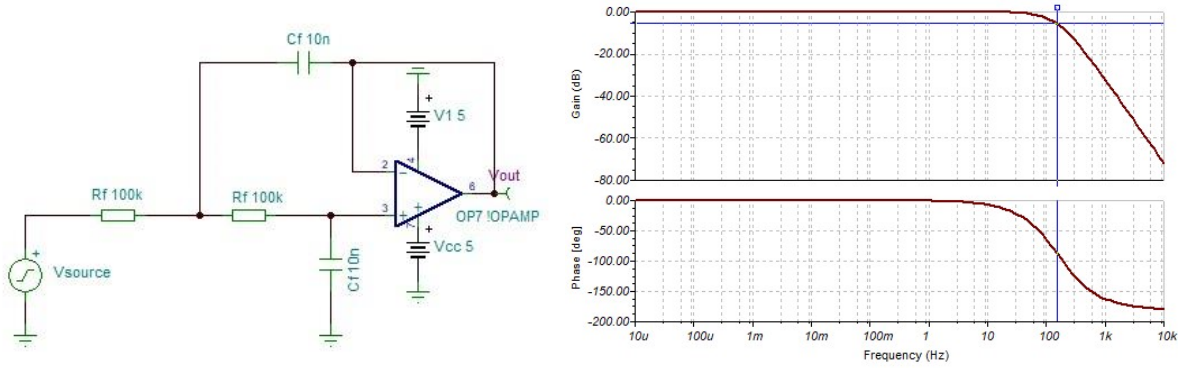

Figure 20: Second order Sallen key Low pass filter. On the right the AC frequency response with the gain (dB) on the y-axis and the frequency (Hz) on the x-axis. The blue line is at 150 Hz with a gain of -5.56 dB

Table 2: The different upper cut-off frequencies for each electrogram, with the selected feedback resistance

Different upper cut-off frequencies for each electrogram			
	Cut-off frequency (Hz)		
Signals	Desired	Set	Resistance (R_f)
Electrocardiogram (ECG)	150	159	100 kΩ
Electromyography (EMG)	500	482	33 kΩ
Electroencephalogram (EEG)	40	40.89	390 kΩ
electrooculogram (EOG)	10	10	1.5 MΩ

3.13 Operational amplifier

The gain of the amplifier concentrates in the first stage of the instrumentation amplifier. That is why the operational amplifiers (op amps) at the input stage determine the input noise. Thus, the required op amp needs to have low input noise.

The biopotential amplifier will be powered by a single supply. That is why another desired feature is a low-power rail-to-rail op amp. The chosen operational amplifier is TLC2274ACN [35]. This is an integrated circuit (IC) that contains four op amps in a Plastic Dual in-line Package or PDIP. In total it has 14 pins with 3 pins for each op amp and one pin for V_{dd+} and one for V_{dd-}.

It has a maximum V_{dd+} of 8 V and a V_{dd-} of minimum -8 V. The input voltage is from V_{dd-} - 0.3 until V_{dd+} which satisfies the rail-to-rail feature as well as being able to function on a single supply. It has a differential and common-mode input resistance of 10^{12} Ω. It also has a low Noise of 9 nV/√Hz at f = 1 kHz.

The choice has been made to use IC sockets for different reasons. The first reason is to protect the IC from overheating during the soldering process. The second reason is to protect the IC pins from bending or breaking during usage, reducing the stress on the pins. A last reason is that the ICs can be changed easily in case of an IC failure or PCB failure, without the need for resoldering. Because the op amp is one of the more expensive components, this last reason is good for the durability and reusability of the circuit.

4 Results

The different stages of the bio amplifier are simulated in the previous chapter. Now, all stages are connected to complete the final design. Each of the chosen electrograms are simulated in TINA-TI to acquire the AC frequency response of the system. If the simulation shows the expected result, a prototype will be designed and built onto a printed circuit board (PCB). This PCB will be tested first with the bio simulator. If the PCB works as expected, the different electrograms will be taken from a test subject.

4.1 Simulations

4.1.1 Electrocardiogram

The first simulation in TINA-TI is for an electrocardiogram. The configuration components such as R_g, R_i and R_f are set for a bandwidth of 0.05 – 159 Hz with a gain of 60 dB. All other components are unchanged during the different electrograms.

The AC frequency response of the biopotential amplifier of an ECG is illustrated in Figure 21 and the AC frequency response is displayed in figure 22. There is a gain of 60 dB in the frequency range of the ECG signals. The gain at the cut-off frequencies of 0.05 Hz is 57.8 dB and at 150 Hz is 54.3 dB.

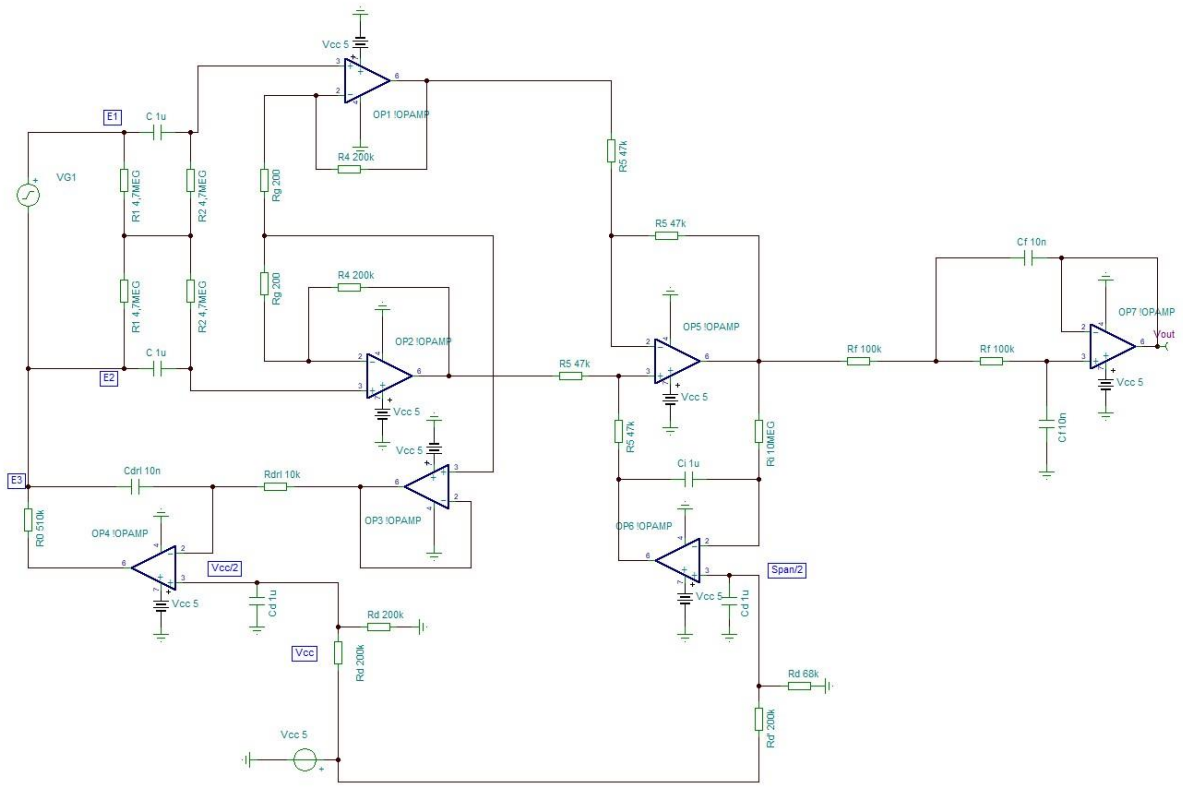

Figure 21: The circuit that is built in TINA-TI. This example has the configurations for an ECG

At the lower frequencies, from 0.01 Hz there is an attenuation slope of 10.8 dB per octave. Another way of measurement is that from this frequency there is an attenuation slope of 38 dB per decade. For the higher frequencies, the rate of attenuation is 11.45 dB per octave at 300 Hz and 38.5 dB per decade from 150 Hz. As a result, the desired signals are amplified by around 60 dB while higher and lower frequencies are attenuated.

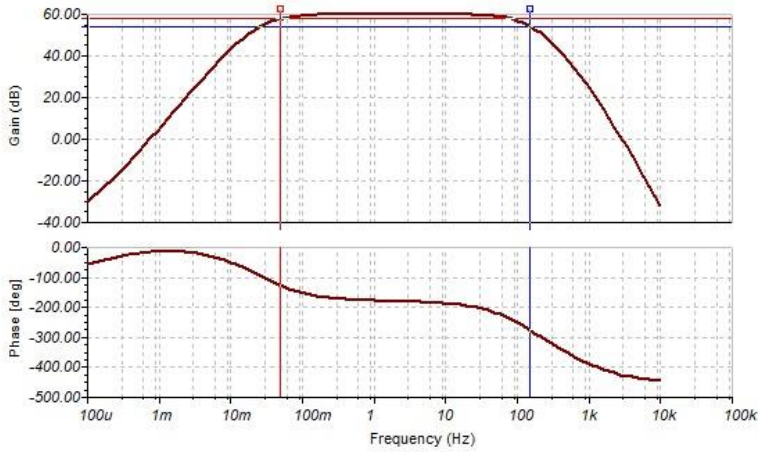

Figure 22: AC frequency response of the electrocardiogram displaying the gain (dB) and phase change (degrees) in function of the frequency in Hz. Red line (a) is at 0.05 Hz at a gain of 57.8 dB. The blue line (b) is at 150 Hz and has a gain of 54.3 dB

4.1.2 Electromyography

The configurations to perform an electromyography, compared with an electrocardiogram, are to change the bandwidth to 20 to 500 Hz. The gain is unchanged and is 60 dB. This configuration requires the low pass filter resistors to be set R_f = 33 kΩ and the integrator resistor R_i = 10 kΩ. The electrical schematic can be found in appendix A.

Figure 23 displays the AC frequency response of the designed circuit. The gain at the cut-off frequencies 20 to 500 Hz is respectively 57.8 dB and 52.6 dB. The attenuation slope at low frequencies is 20 dB per decade or 6 dB per octave. This corresponds to the attenuation of a first order filter. At higher frequencies an increasing attenuation slope is simulated, starting from 47 dB per decade at 500 Hz up to 58 dB per decade at 4 kHz.

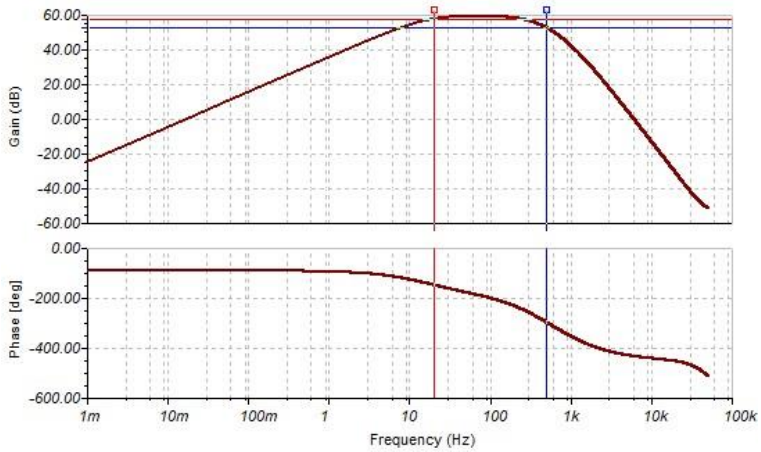

Figure 23: AC frequency response of the electromyography displaying the gain (dB) and phase change (degrees) in function of the frequency in Hz. Red line (a) is at 20 Hz at a gain of 57.8 dB. The blue line (b) is at 500 Hz and has a gain of 52.6 dB

4.1.3 Electrooculogram

To perform an electrooculogram, a bandwidth of 0.05 to 10 Hz is set with a gain of 60 dB. The feedback resistors of the low pass filter need to be changed to R_f = 1.5 MΩ. The electrical schematic is shown in appendix B.

The graph in figure 24 displays the simulated AC frequency response of the circuit. The cut-off frequencies of 0.05 Hz and 10 Hz respectively have a gain of 57.7 dB and 54.3 dB. The attenuation slope at low frequencies is 38 dB per decade or 11.6 dB per octave. At high frequencies, the attenuation slope increases from 33.5 dB per decade at 10 Hz to 57.3 dB per decade at 1 kHz.

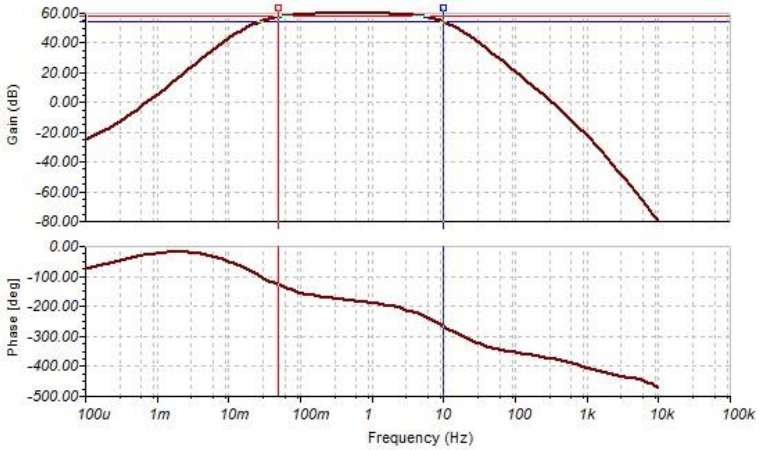

Figure 24: AC frequency response of the electrooculogram displaying the gain (dB) and phase change (degrees) in function of the frequency in Hz. Red line (a) is at 0.05 Hz at a gain of 57.7 dB. The blue line (b) is at 10 Hz and has a gain of 54.3 dB

4.1.4 Electroencephalogram

The signals of an electroencephalogram have the lowest amplitude. For this reason, a gain of 2001 or 66 dB is chosen. The gain resistors are configured to R_g = 100 Ω. The cut-off frequencies are 0.05 – 40 Hz, thus R_f = 390 kΩ. The AC frequency response is shown in figure 25 and the electrical schematic is shown in appendix C.

The gain at the cut-off frequencies is 63.7 dB at a frequency of 0.05 Hz and 59.9 at 40 Hz. The attenuation slope at low frequencies is 38.1 dB per decade from 0.005 Hz or 11.6 dB per octave. For high frequencies a slope of -36.0 dB per decade is simulated.

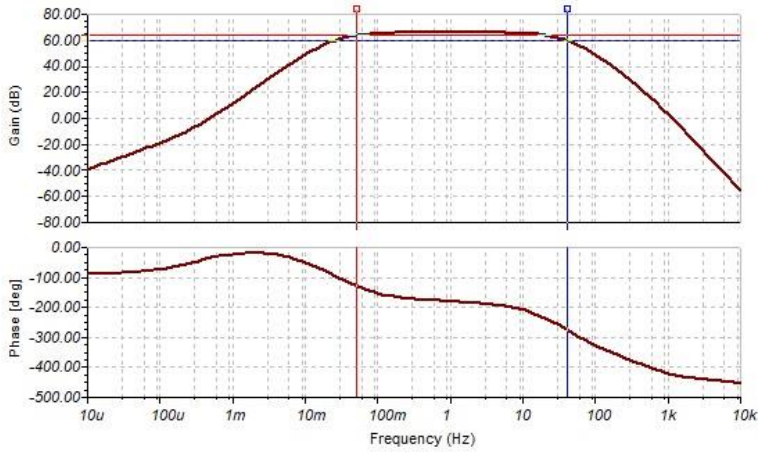

Figure 25: AC frequency response of the electroencephalogram displaying the gain (dB) and phase change (degrees) in function of the frequency in Hz. Red line (a) is at 0.05 Hz at a gain of 63.7 dB. The blue line (b) is at 40 Hz and has a gain of 59.9 dB

4.2 Prototype design

The simulations of the selected electrograms display the expected results. The next step in this research is to design and build a printed circuit board (PCB). Two different designs are created using Kicad 6.0. The first PCB design is the most basic, where no configurations can be made to the board. The only way changes of bandwidth or gain can be made, is by resoldering components. This design fulfils the requirements of the thesis and has the lowest cost for a single electrogram. The second PCB design includes headers to configure the bandwidth and gain of the amplifier. Jumpers are used to select the desired resistors by placing them on the headers. This design results in a lower cost when different electrograms need to be performed, where one board equals four basic design boards.

The first requirement of the PCB was that it has dimensions of 50 x 100 mm on a 2 layered PCB. The input signal is delivered by a 3.5 mm jack male cable. Thus, the first component is a female mini-jack receiver. A horizontal mounted jack is chosen above the smaller, vertical mounted jack. The only reason for a component with a bigger surface is because this is more robust, which was another criterion of this PCB. The second requirement was to work with only DIP components for easier soldering and later modification of the bio amplifier.

The output signal will be received by the Biopac MP35 through a DB9 cable. For this reason, a D-sub 9 pin connector is employed which will receive the output while also delivering power to the device. In this design, the positive potential of the input signal is connected to resistor $R_{1,2}$, the negative potential is connected to $R_{1,4}$. When referring to the electrode wires, the yellow electrode is the positive potential, the red electrode the negative and the green electrode is the reference.

4.2.1 Basic design

The design in Kicad starts with a schematic of the circuit as displayed in figure 26. This schematic is necessary to create nets. A net is the electrical connection of components, sources and wires. If one pole of a capacitor belongs to a net, it is impossible to connect this to another net. This system prevents the user from making unwanted connections between traces and components.

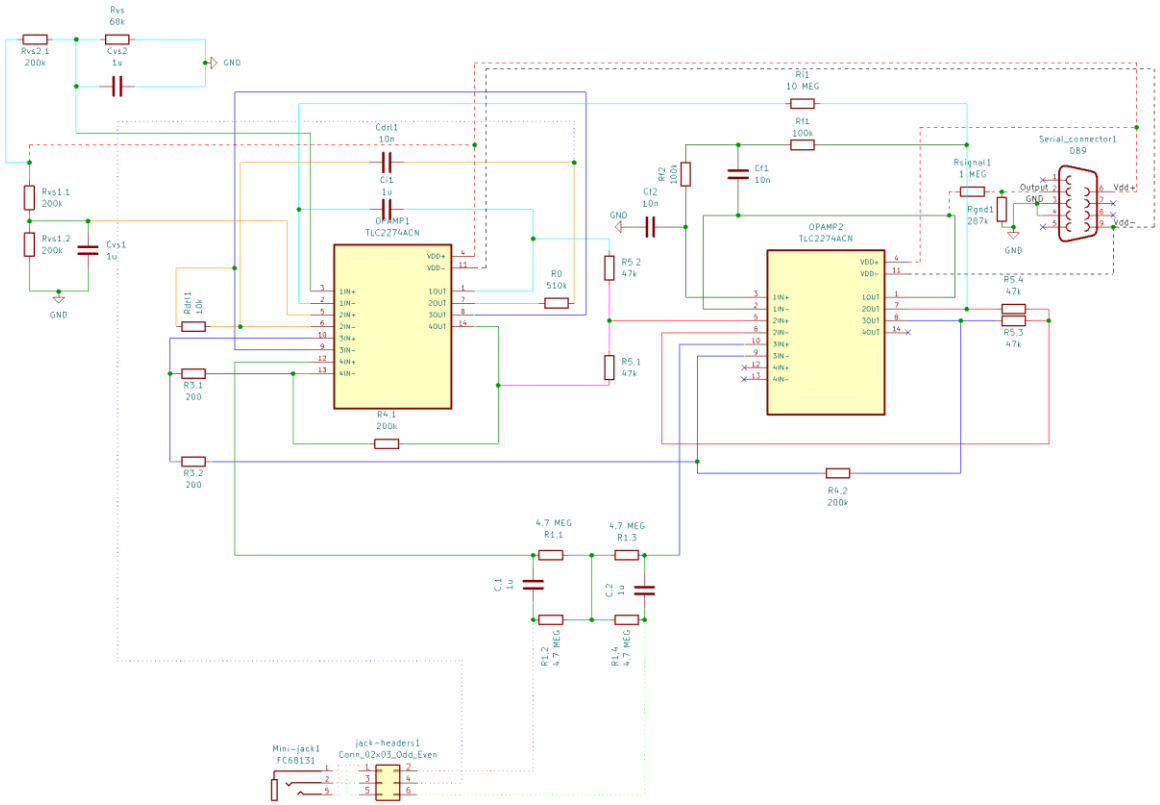

Figure 26: Kicad schematic of the basic design

The schematic uses the component values for an electrocardiogram, but during the soldering of the PCB these values can be changed to the desired configuration for other electrograms. The mini-jack connection is placed at the bottom of the schematic. The connection between the mini-jack and the headers is based on the footprint of the actual PCB design. The headers are connected to the inputs respectively electrodes 1, 2 from the electrical circuit. Electrode 3 is the reference electrode, or driven right leg.

A voltage splitter is created between the output of the bio amplifier and the output through hole that connects to the MP35. The voltage splitter divides the output signal by 5, where the signal resistor R_{signal} = 1 MΩ and the ground resistor R_{GND} = 287 kΩ.

The PCB design is illustrated in figure 27. The ground plane is removed in this illustration for better readability, but in the actual design there is one present on the back plane. The red traces are on the front plane while the blue traces are on the back plane.

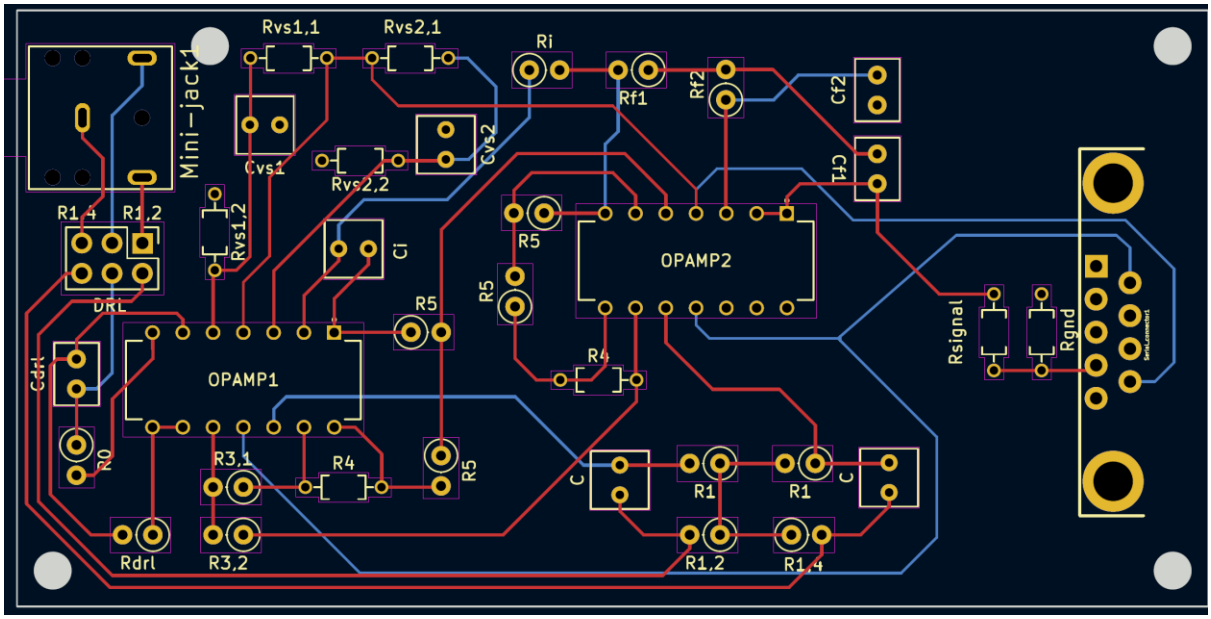

Figure 27: PCB design of the basic prototype without ground plane

The headers below the mini-jack connector, on the left side of the image, are placed for the possibility to connect a simulator to the bio amplifier. When jumpers are placed on all three headers, the mini-jack connector is the input port.

The path width of all traces is the standard of 0.25 mm. The variables to calculate the trace width are the maximum current, copper thickness, ambient temperature, temperature rise and the trace length. The op amp has a maximum input or output current of 50 mA, and the thickness of the copper layers is 0.2 mm. The ambient temperature for the calculation is 25°C and a temperature rise of 20°C. The maximum trace length is drawn for V_{cc-} at around 120 mm, so for the calculation 150 mm is used. When using PCBway PCB trace width calculator [36], the required trace width is 0.0032 mm. Thus, the standard trace width of 0.25 mm is more than sufficient.

4.2.2 Configurable design

This is a more complete design for a biopotential amplifier that can perform different electrograms without the need for resoldering components. The electronic schematic is shown in figure 28. Two 2x4 headers are placed to select the feedback resistance for output 1 and inverting input 1 of op amp 2, or in other words the feedback resistors for the Sallen Key low pass filter. The four resistor values of 100 kΩ, 1.5 MΩ, 33 kΩ and 390 kΩ for respectively the ECG, EOG, EMG and EEG are selectable by changing the jumpers on the headers.

Two 2x2 headers are used to select the gain resistors for a gain of 1001 or for 2001. At last, one 2x2 header is added to select the integrator resistance R_i to select the lower cut-off frequency. The remaining components remain unchanged compared to the basic design.

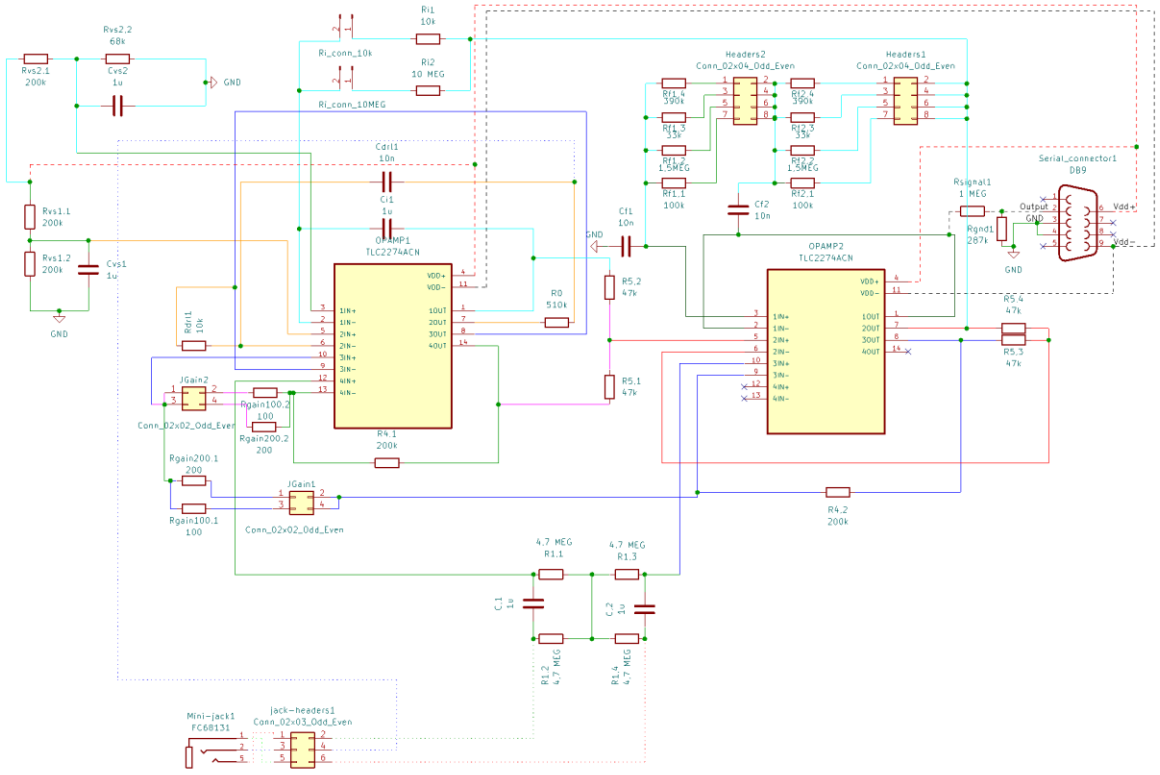

Figure 28: KiCad schematic of the configurable circuit

The notes and design choices for the previous, basic design are also applicable for this design in figure 29. The ground plane is again removed to make the design choices clearer. In the actual design the ground plane is added on the back. The final result of the PCB is shown in Figure 30. All components are soldered onto the board and the jumpers are placed to receive an ECG signal through the mini jack.

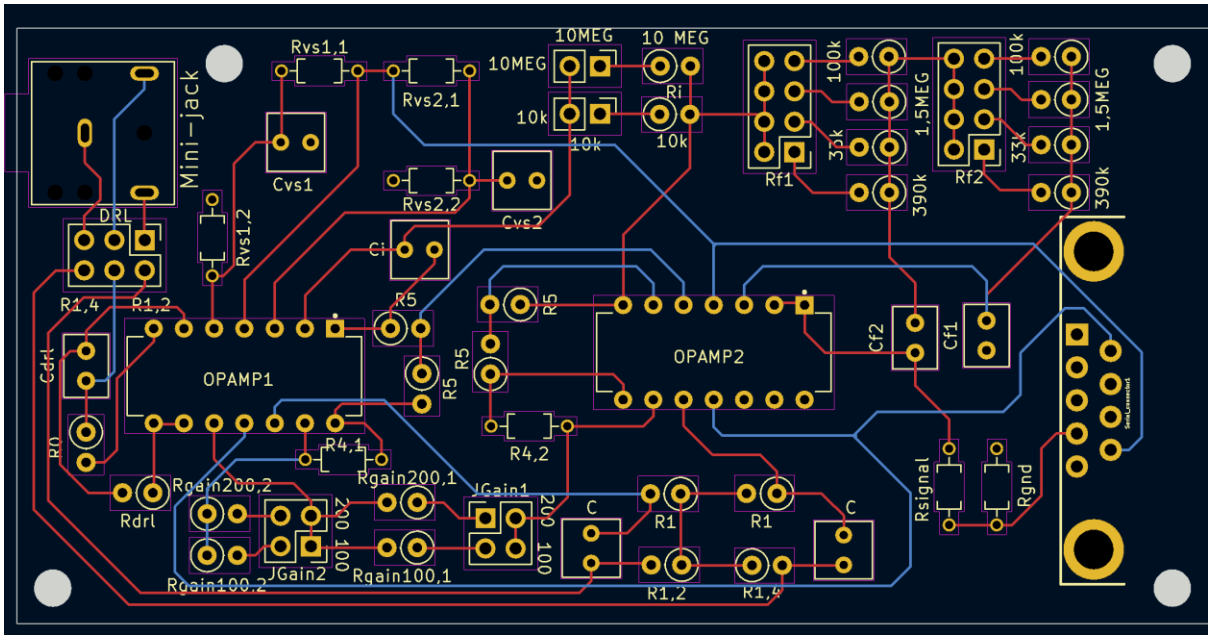

Figure 29: The PCB design for the configurable design without a ground plane

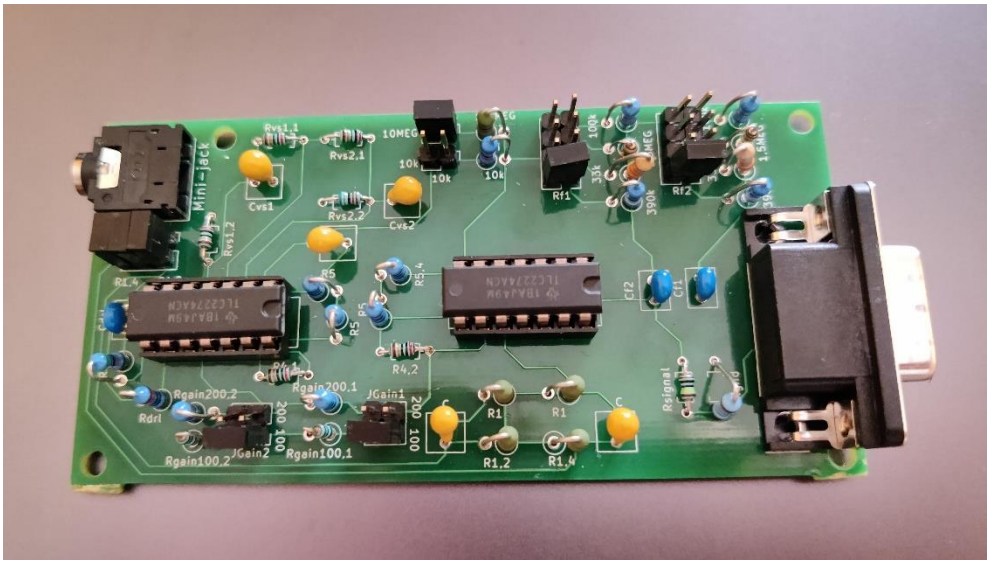

Figure 30: Configurable design with all components soldered. The jumpers are configured to receive an ECG signal through the mini jack

4.2.3 Combined design

The final design is the two previous designs combined into one 100 x 100 mm design. A horizontal slot is routed in the middle of the PCB to facilitate the separation to their original designs. Figure 31 illustrates the ordered PCB layout. The layout designed in Kicad is shown on the left and the delivered result is shown on the right image. The board is later separated into two equally sized PCBs of 50 x 100 mm. The 3D render can be found in appendices D and E.

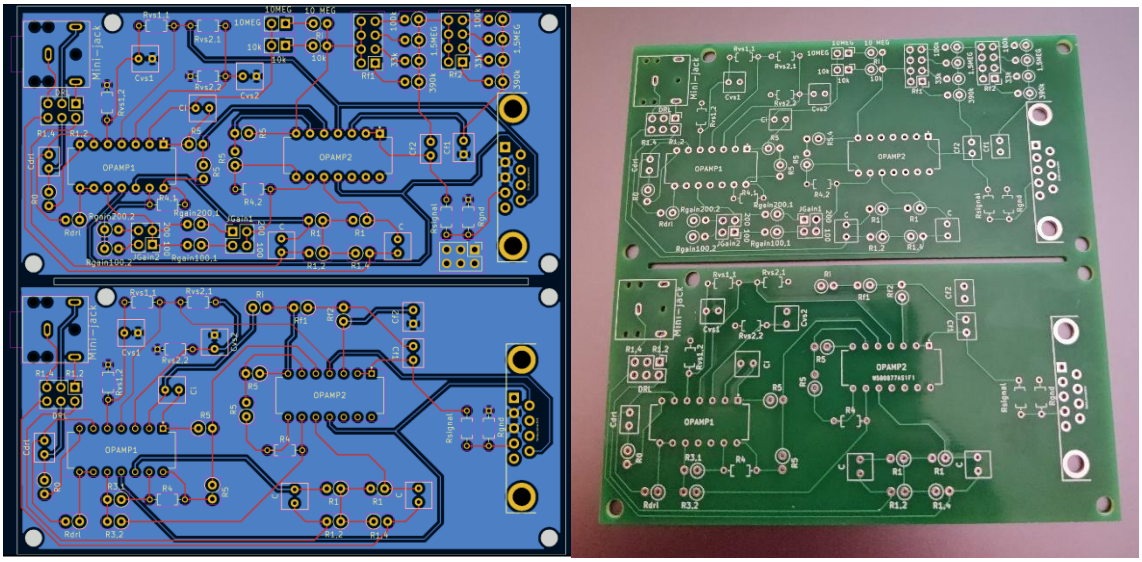

Figure 31: Final prototype design, the two designs combined onto one board

4.3 Powerline interference

The testing of the designed PCB is done in the laboratory of the university. The V_{cc}+ and the ground of the PCB are connected to a DC power supply that is not delivering power. Figure 32 displays the powerline interference when an oscilloscope is connected to the output pin and to the ground of the PCB. The input pins are floating, or in other words not receiving a signal. The oscilloscope measures a signal of 210 mV at 50.30 Hz.

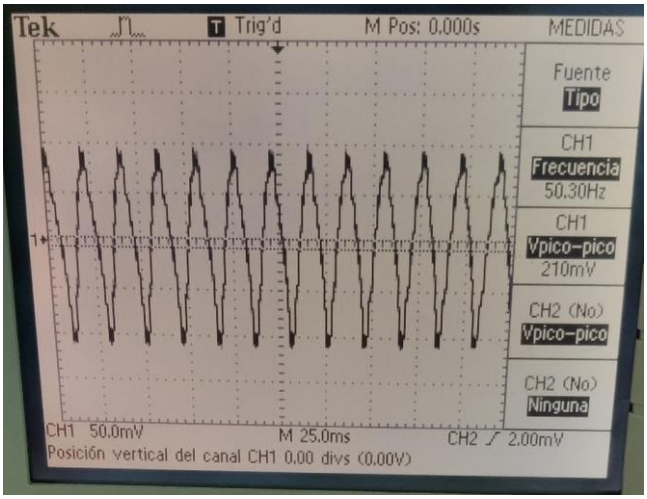

Figure 32: Powerline interference of 200 mV at 50 Hz when the oscilloscope is connected to the PCB. The PCB is connected to a 5 V power supply that is not delivering power at the moment of this picture

4.4 Bio simulator test

The bio simulator recreates an artificial heart signal. It has a positive output V+ and a lower positive output V-. Both outputs are positive voltages, but V+ has a bigger amplitude. When the V+ and V- of the bio simulator are directly connected to an oscilloscope, an ECG signal as illustrated in figure 33, is the result. The signal has a peak-to-peak amplitude of around 7 mV, with noise of around 2 mV. The P-wave, QRS complex and T wave can be distinguished, but the noise makes it imprecise.

The expectation is that the bio amplifier will amplify the differential signal while removing the noise. This should result in a cleaner output, where the signal-to-noise ratio is improved.

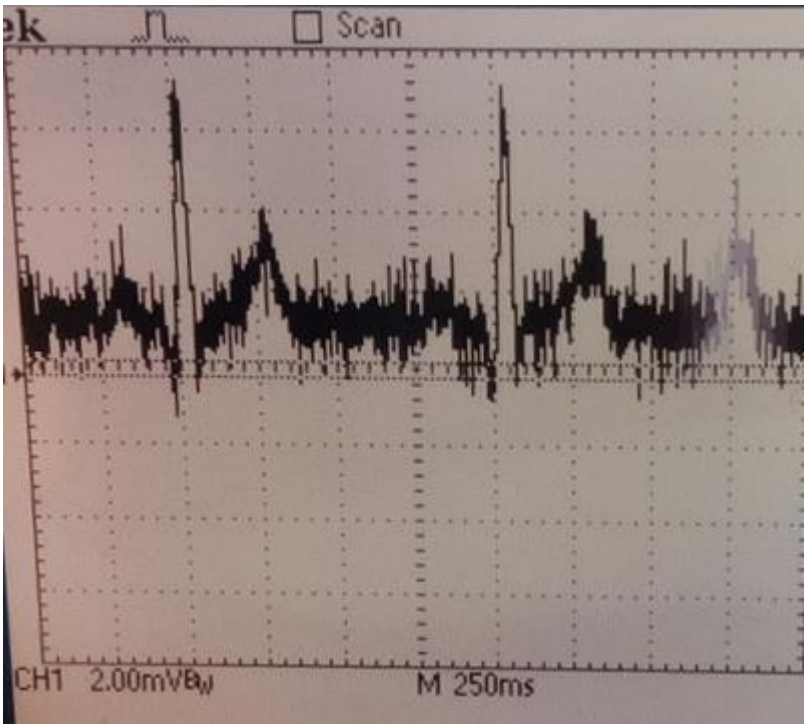

Figure 33: Output of the bio simulator on an oscilloscope without the usage of the bio simulator

4.4.1 Pre-testing

The working of the PCB is first pre-tested on an Arduino Uno and oscilloscope to validate the correct working of the amplifier, before using the Biopac MP35. The configuration settings of the biopotential amplifier are set to receive an ECG signal. However, the peak-to-peak amplitude of the bio simulator is six times larger than that of a real ECG signal. For this reason, R_{gain} = 2.2 kΩ to realize a gain of 92.

The working of the bio potential amplifier is tested by connecting the output of the PCB to an analog input of an Arduino Uno first. Figure 34 illustrates the read out of the ECG signal. The DC offset is around 1080 mV and even though there is noise present, the P-wave, QRS complex and T wave are

distinguishable. The peak-to-peak amplitude is around 600 mV. This confirms that the biopotential amplifier can amplify the ECG signal while not amplifying the noise.

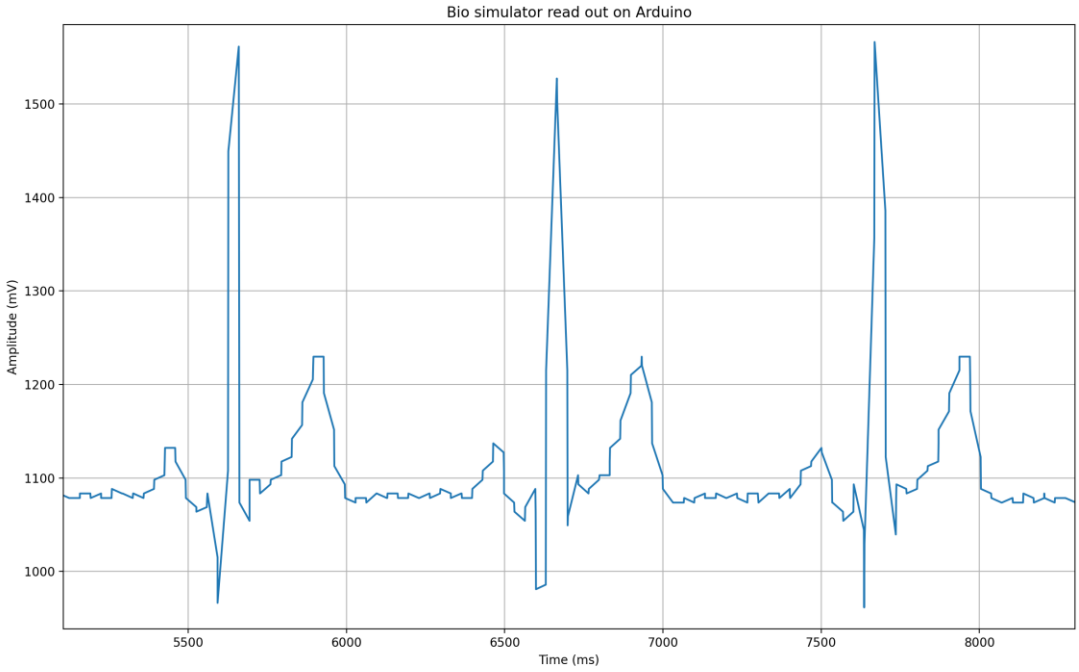

Figure 34: The signal of the bio simulator amplified by the designed biopotential amplifier received by an analog input of the Arduino Uno. The amplitude (mV) on the y-axis and the time (ms) on the x-axis

Figure 35 displays the amplification of the bio simulator by the designed biopotential amplifier on an oscilloscope. The positive input of the oscilloscope is connected to the output of the bio amplifier, before the voltage divider. Thus, the output directly corresponds to the settings of the bio amplifier. The settings of the oscilloscope on the left picture are horizontal 250 ms/division and vertical 500 mV/division. The right picture has the same horizontal scale, but the vertical scale is set to 250 mV/division with a DC offset of 1.25 V.

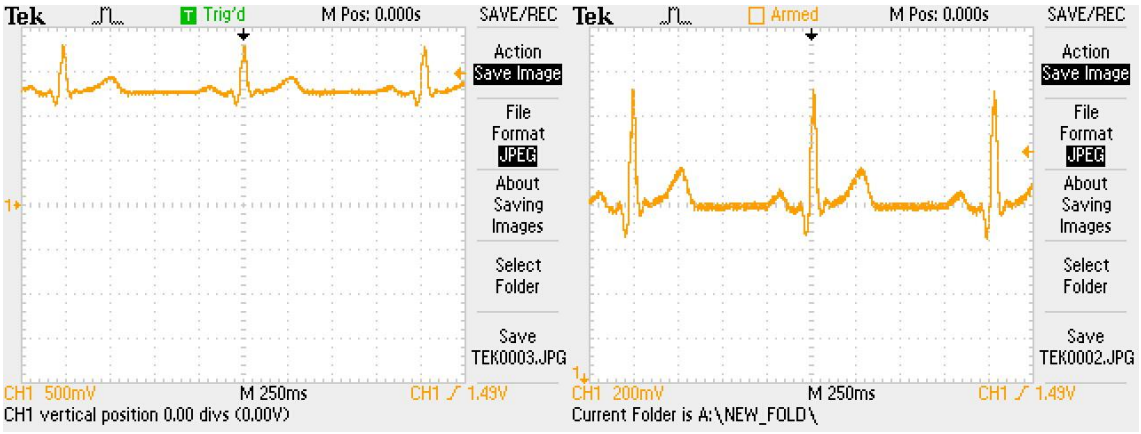

Figure 35: The output of the bio simulator with a gain of 92. The amplitude (mV) on the y-axis and the time (ms) on the x-axis. The left graph has 500 mV/division while the right picture has 200 mV/division with an offset of 1.25V

The peak-to-peak amplitude is around 600 mV. This is in line with the expectation of an amplification of 92 for an input signal of around 7 mV.

The ECG signal shows some noise, but the P-wave, QRS complex and T-wave are distinguishable. When the horizontal scale is lowered to 100 ms/division or one period of the ECG, it shows that the noise is the powerline interference at a frequency of 50 Hz. When averaging of the signal is applied, the 50 Hz noise is removed, resulting in a clean signal, illustrated on the right graph of figure 36.

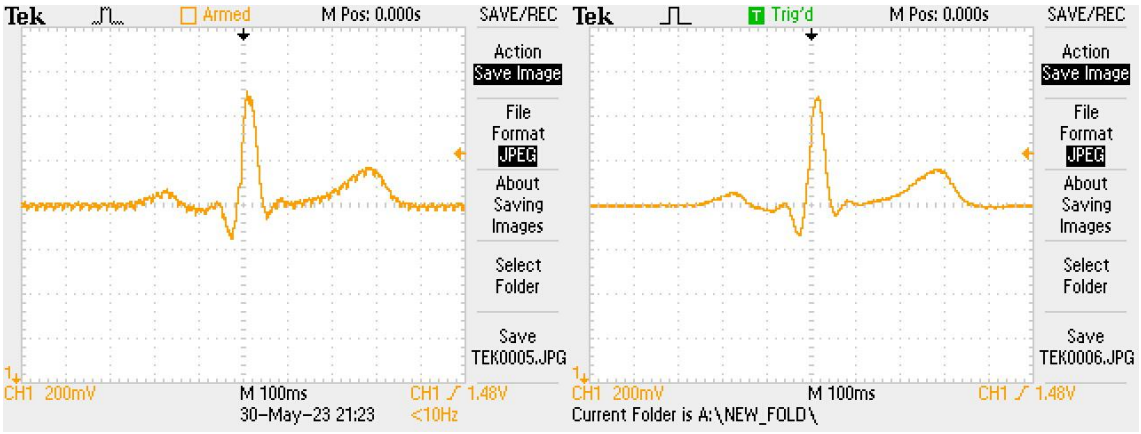

Figure 36: The amplified ECG signal with a horizontal scale of 100 ms/division and a vertical scale of 200 mV/division. The left graph is a sample, the right graph uses averaging

4.4.2 Biopac MP35

Figure 37 illustrates the graph for an amplification of the bio simulator with a gain of 400 on the Biopac MP35. The gain is raised from 92 to around 400 by replacing the gain resistance to R_{gain} = 500 Ω. The

whole output of the biopotential amplifier is divided by 5, resulting in a DC offset of 240 mV instead of 1.2 V. The peak-to-peak amplitude is around 460 mV, or amplified by 5 a peak-to-peak of 2.3 V.

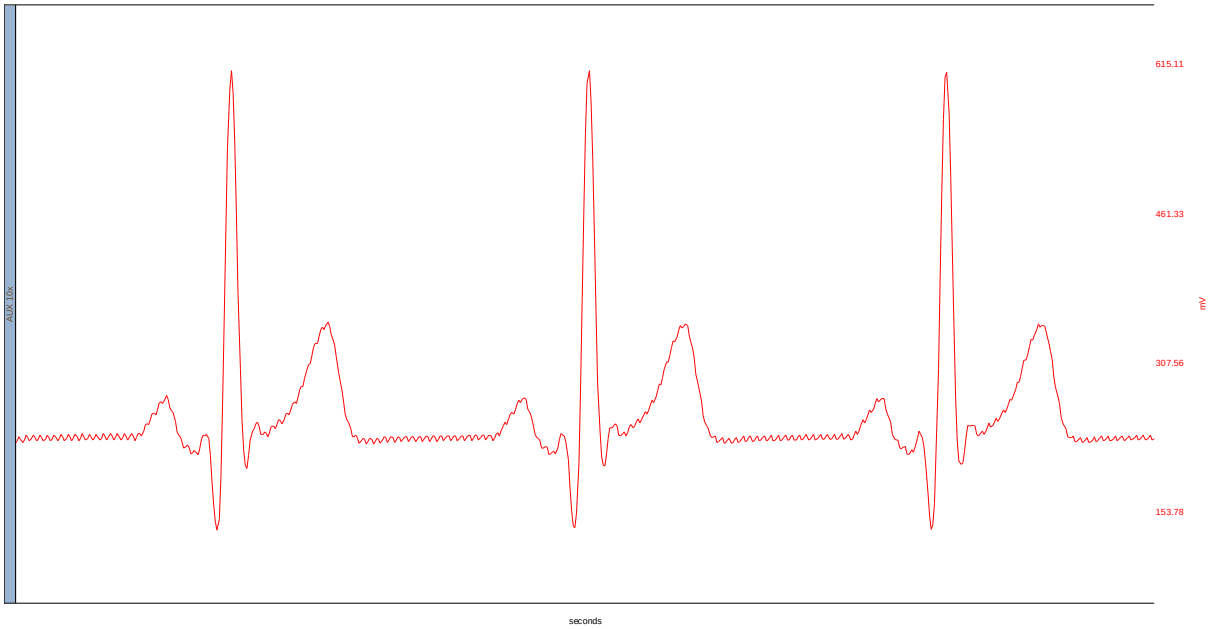

Figure 37: Amplification of bio simulator by the biopotential amplifier with a gain of 400. The amplitude (mV) on the y-axis and the time (seconds) on the x-axis. No digital filters are applied

4.5 Test subject

After the successful simulations of the circuit and successful tests of the bio simulator, the biopotential amplifier is used on a test subject. The first electrogram will be an electromyography of the bicep. After this, an electrocardiogram is taken, followed by an electrooculogram. The sample rate of the Biopac is standard 200 samples per second, unless noted otherwise.

4.5.1 Electromyography

The electromyography is taken of the bicep of the test subject. The electrodes are placed as shown in figure 38. The positive potential is at the bottom of the bicep and the negative potential is at the top of the bicep. The reference electrode is placed on the elbow. The gain for this measurement is 1001 with a bandwidth of 20 – 500 Hz. For this measurement, a sample rate of 1000 samples per second is

applied to avoid aliasing. The built-in band stop filter of 50 Hz is used for both the raw signal and the filtered value.

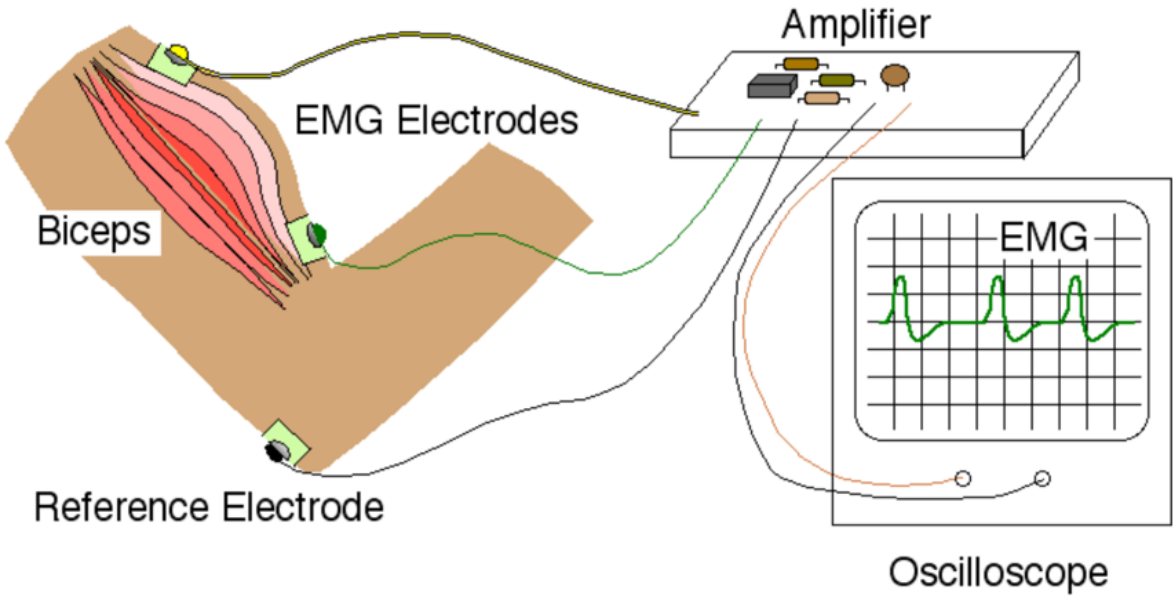

Figure 38: Position of electrodes placed on the bicep for an electromyography [37]

The raw signal is displayed in the red graph in figure 39. The measurement is taken over a period of 50 seconds. The DC offset of the electromyography is 250 mV. A peak is the result each time the bicep is bent. The peak-to-peak amplitude depends on the force and speed of the bending of the bicep. The more force is applied, the higher the amplitude. In this measurement, the highest peak-to-peak amplitude is measured at 500 mV in the Biopac MP35. This is the measurement after the voltage divider with a division of 5, so the peak-to-peak is around 2.5 V. The potential difference on the bicep itself is around 2.5 mV.

After the measurement, the baseline is removed and a root mean square over 40 samples is taken to remove noise, resulting in the blue graph of figure 39. The peak amplitude of the bicep contractions varies between 50 mV and 200 mV.

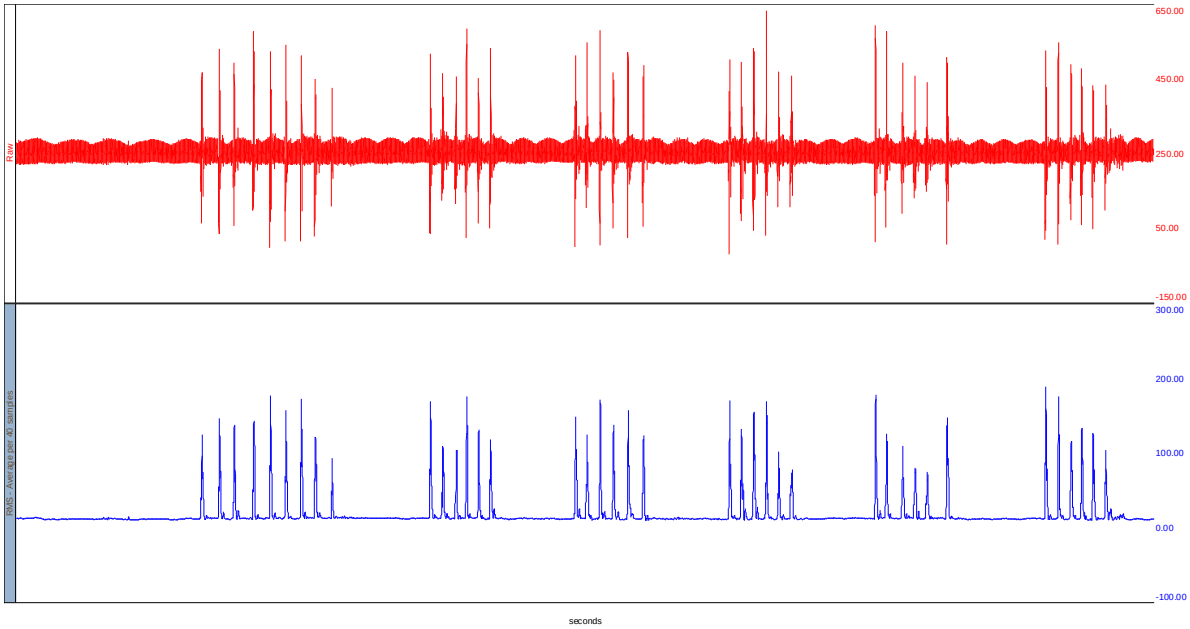

Figure 39: The graph of EMG output with the amplitude (mV) on the y-axis and the time (seconds) on the x-axis. The red (top) graph is the raw EMG signal measured from the bicep and in blue (bottom) the RMS and average filtered per 40 samples with sample rate of 1000 samples per second. A digital 50 Hz stop band filter is applied. The duration of the measurement is 50 seconds.

4.5.2 Electrocardiogram

The graphical recording of the test subject his heart is taken. The electrodes are placed as in figure 40. The positive potential is received at the left lower rib cage, under the heart. The negative potential electrode is placed on the top of the ribcage and the reference electrode is placed on the right side of the ribcage.

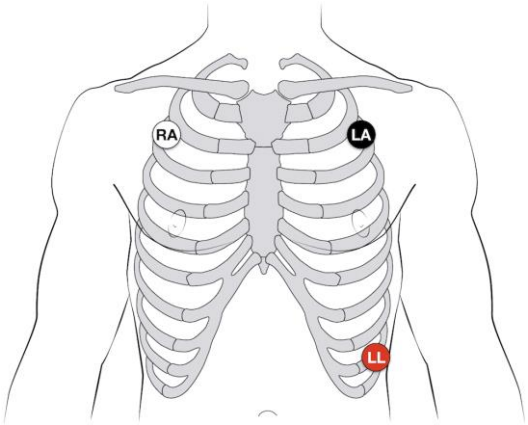

Figure 40: Electrode placement for an electrocardiogram [38]

Figures 41, 42 and 43 illustrate the amplification of the heart signal of a test subject. The gain is set at 1001 or 60 dB. The DC offset measures 260 mV or 1.3 V. The peak-to-peak amplitude is measured at 700 mV after the voltage divider.

When a working phone or laptop is placed close to the PCB, in the example illustrated in figure 42, in a radius of 50 cm, the noise at the output is significantly larger than if powered devices are outside this range. The noise difference can be up to 200 mV at the input of the MP35. The noise is powerline interference because it has a frequency of 50 Hz. When the built-in digital band stop filter of the MP35 is used, a clear signal is obtained, as illustrated in figure 43.

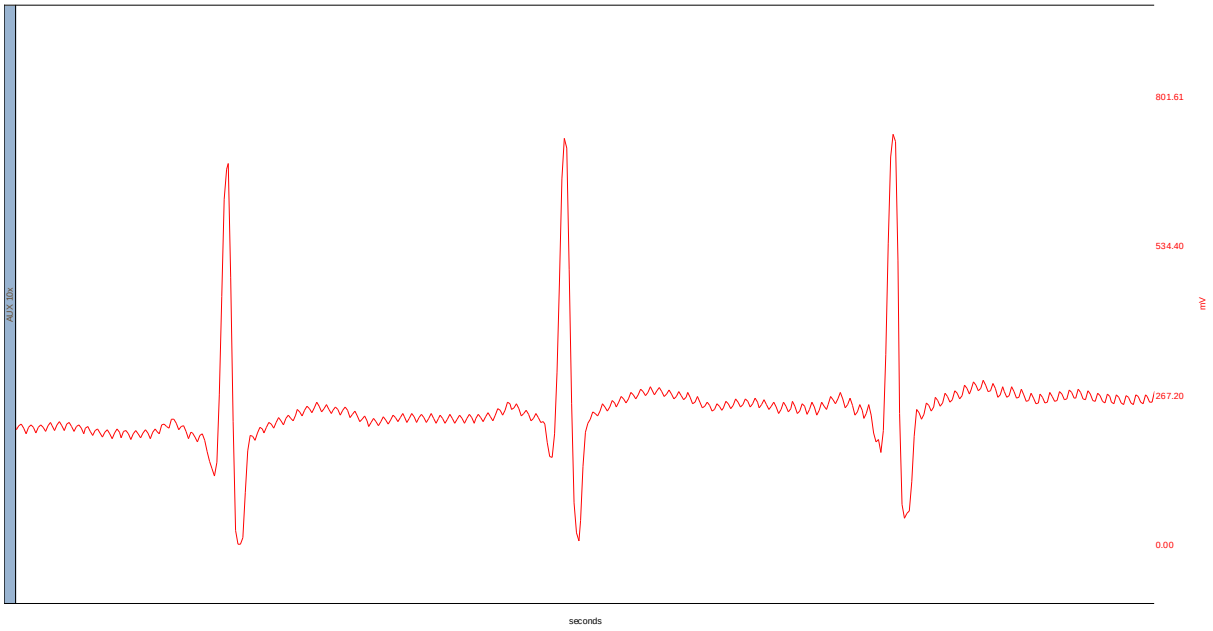

Figure 41: Heart signal amplified by 1001, no band pass filter applied from the Biopac MP35. The amplitude (mV) on the y-axis and the time (seconds) on the x-axis

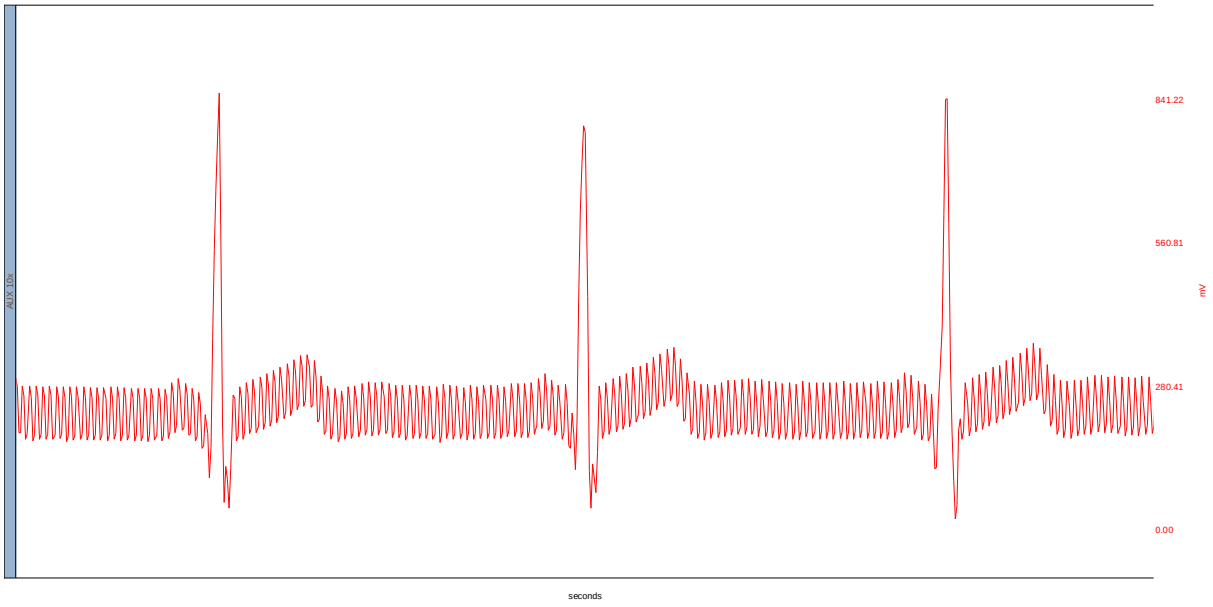

Figure 42: Heart signal amplified by 1001 with an electronic device close to the PCB. The amplitude (mV) on the y-axis and the time (seconds) on the x-axis

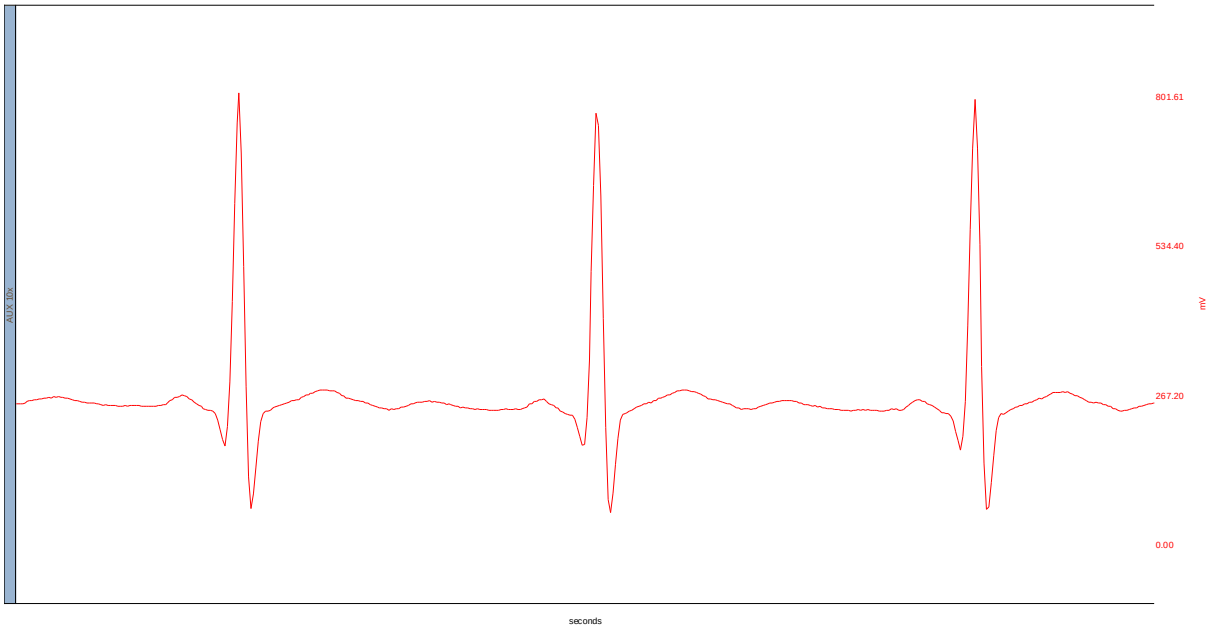

Figure 43: Heart signal amplified by 1001 with the usage of Biopac MP35 band stop filter at 50 Hz. The amplitude (mV) on the y-axis and the time (seconds) on the x-axis

4.5.3 Electrooculogram

The electrodes for the electrooculogram are placed horizontally left of the left eye, and right of the right eye. The reference is placed in between the two eyes on the forehead. First, the positive potential is placed at the right eye and the negative potential is placed at the left eye. For this test, no digital filters of the MP35 are used.

When the test subject looks to the positive potential side, a rise in the potential is measured. When the subject looks to the negative potential side, a drop in potential is measured. In figure 44, the measurement starts when the subject is looking to his right. This is displayed as a rise relative to the DC offset. This move is followed by looking straight ahead, where the signal goes back to the DC offset. The drop in potential signifies that the subject looks to his left, almost resulting in an output of 0 V. In the final stage of the test, the subject looks straight ahead and blinks repeatedly. This usage of the muscles is also caught by the electrodes but has a significant lower amplitude.

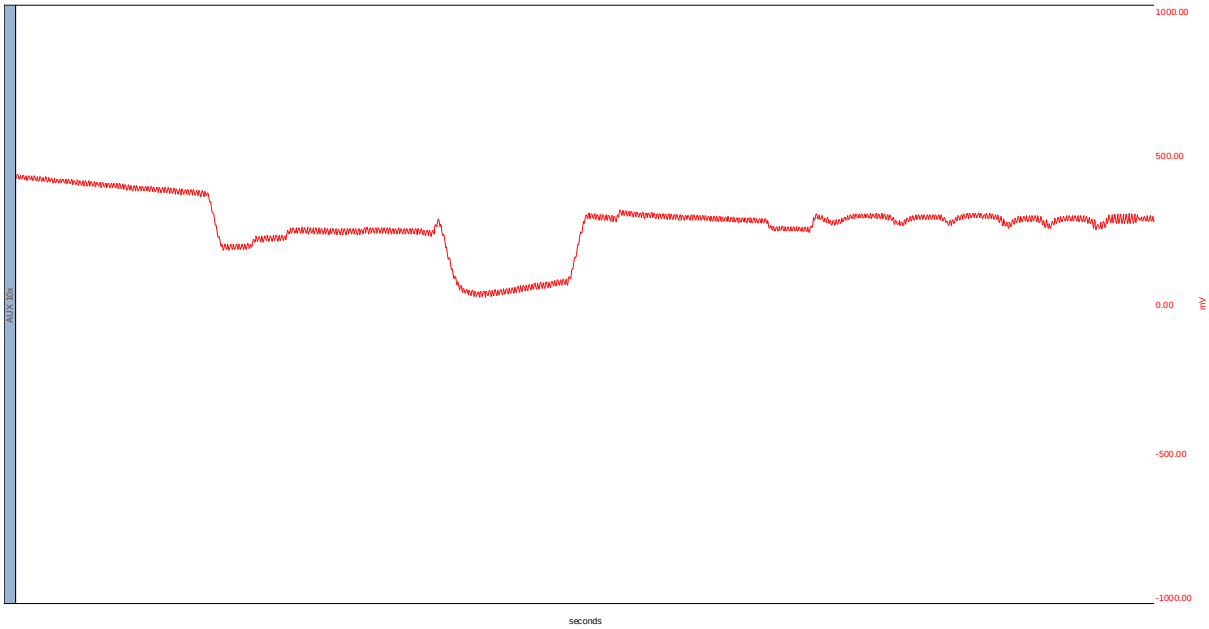

Figure 44: Electrooculogram of horizontal view. The amplitude (mV) on the y-axis and the time (seconds) on the x-axis. The test subject looks to the right at beginning of the measurement, followed by looking forward, then left. The measurement finishes after blinking the eyes repeatedly

5 Discussion of results

5.1 Simulations

The simulations of the biopotential amplifier gave the expected results as calculated. The lower cut-off frequency could be chosen higher, around 0.05 Hz as required. However, the Biopac MP35 has a built-in high pass filter of minimum 0.05 Hz, so this is no problem when reading out the output. The upper cut-off frequencies of the different electrograms are set close to their desired values, where the biggest deviation is for ECG with an upper cut-off frequency at 159 Hz instead of 150 Hz. Testing revealed that this did not pose a problem.

5.2 Bio simulator test

The amplification of the bio simulator is tested on three different readout devices namely an Arduino Uno, an oscilloscope and the Biopac MP35. Although all results were as expected, the Arduino uno and the oscilloscope had to be connected to the output signal before the voltage divider. If the output signal was used after the voltage divider, the signal-to-noise ratio was bad.

This is because the amplitude of the noise did not change, but a division of 5 on the desired signal had an impact on readability. For example, a noise of around 20 mV on a peak-to-peak amplitude of 600 mV is a signal-to-noise ratio of 30. When the peak-to-peak amplitude is divided by 5, resulting in a peak-to-peak of 120 mV, with the same noise of 20 mV, results in a signal-to-noise ratio of 6. For that reason, the gain of the bio amplifier was set to 400 instead of 92 for the testing on the Biopac MP35.

The Arduino Uno provides a low-cost option to read-out the output signal of the bio amplifier. To visualize the data better, an amplification of 4.88 is added in the code to create a graph between 0 and 5000. It is possible to generate a live graph of the signal using the built-in serial plotter of Arduino. Another option is to save the data through a python script, using the serial and csv libraries that writes the data to a comma separated values file. Later, the data can be displayed using matplotlib to create the graph. Although the accuracy is 4.88 mV, thus lower than that of an oscilloscope or the MP35, the different waveforms like P-wave, QRS-complex and T-wave were distinguishable. With the data saved in a comma separated values file it is possible to filter out the noise or get the real voltage values to do further calculations.

The last usage of the bio simulator was to test the connections of the DB9 connector to the Biopac MP35. The result of this test was the realization that the selected footprint of the DB9 output cable was a mirrored version of the required one. The selected footprint was for a DB9 male connector, but a DB9 female connector was ordered. There are two ways to resolve this issue, the first one is to order male connectors. The second option is to take a male-to-male DB9 cable and cut it in half and then resolder the connections in the right order. This last option is chosen because the Biopac delivers a - 5 V on V_{cc}-, where a ground connection is required in this design. With this solution, the V_{cc}- cable is left cut and the V_{cc}- pin on the PCB is shorted to ground.

5.3 PCB prototype design

The design of the biopotential amplifier on the PCB was overall a success. The basic design, the one without the possibility to configure the bandwidth or gain, turned out to be too basic. It is a disadvantage to resolder components every time a different electrogram is performed. So, a dedicated

board for one electrogram is possible, but the possibility to configure the bandwidth or gain by changing the jumpers turned out to be a better design choice.

The solution to cut the DB9 cable in half and resolder the wires is not ideal in the powerline interference and general noise shielding. Not only that, but with the intention that this board will be used by multiple students, it is better to be able to use a standard cable without the need for modifications. A new PCB is designed to solve this problem, resolve some smaller mistakes and add more features, as discussed in the section below.

5.3.1 Proposed adjusted design

The mirroring of the DB9 connector cannot be seen in the electrical schematic, which can be found on the right of figure 45. This problem is solved by changing the footprint of the device from a male connector to a female connector. The pin of V_{dd}- at the connector has been disconnected because this pin receives a DC voltage of -5 V. The V_{dd}- of the op amps are directly connected to the ground as a consequence. Again, the PCB design in figure 46 does not include the ground yet, for readability reasons, but this was added on the back plane.

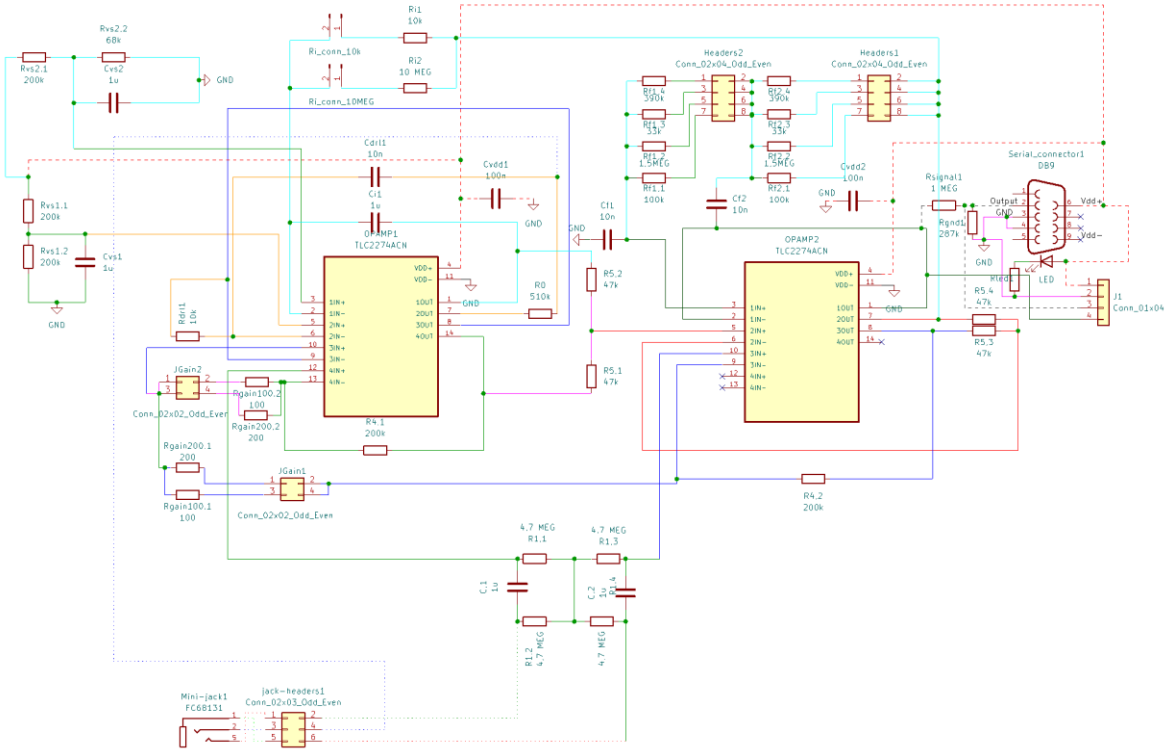

Figure 45: Electrical schematic of the improved PCB design

Another issue of the PCB design is that there are accessible probing points available once the DB9 connector is soldered to the board. As a solution, 4 headers are placed to be able to connect to V_{dd}, ground and the output for both before and after the voltage divider. These headers are placed close to the DB9 connector, as shown in figure 46. There are also 2 headers placed on the bottom left of the board, to be able to measure the raw input signal received by the mini jack. This makes it easier to compare the raw input signal with the amplified result, or to provide an input signal from a different source.

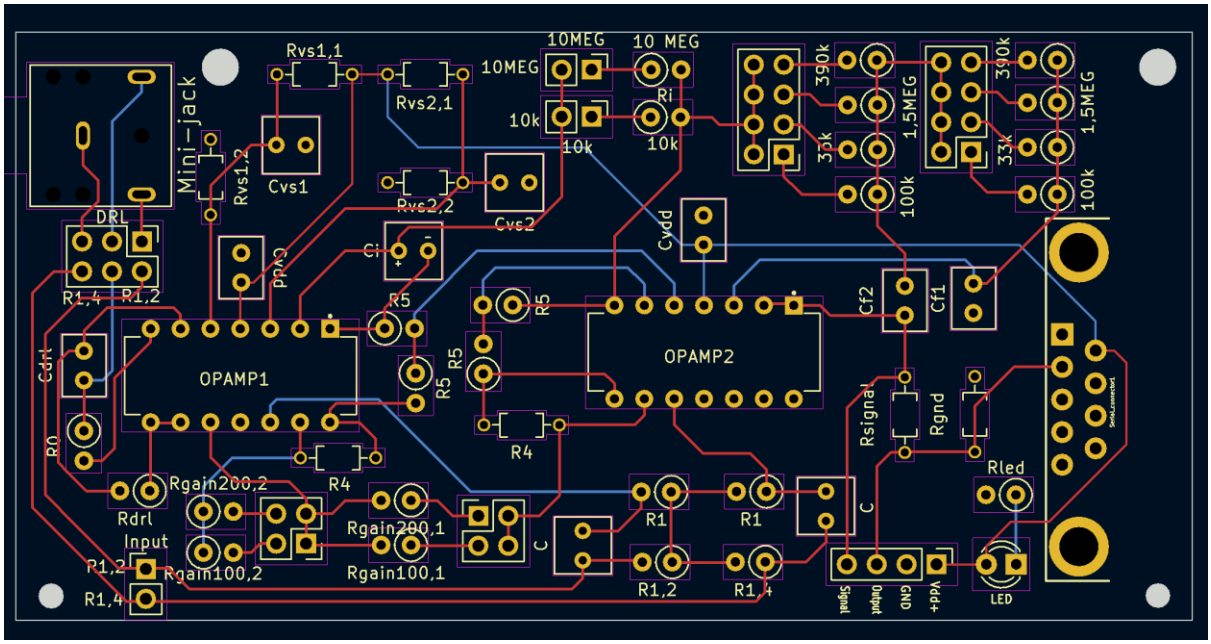

Figure 46: PCB design of the improved board

The next adaptation is for the convenience of the user of the biopotential amplifier. A Light Emitting Diode is placed between V_{dd} and ground to indicate to the user that the board is powered on or off.

A decoupling capacitor is placed at the two V_{dd}+ ports of the op amps. These capacitors are placed as close as possible to the input pin to provide a low-impedance path for high frequency noise on the DC voltage. This noise can affect the performance of the op amp which can result in more noise at the output [39]. A ceramic capacitor with a value of 100 nF is chosen, as given in the application of the op amp in the datasheet [35, p. 26].

Only the configurable PCB design is updated to the improved version because this board is in general more complete in comparison to the basic design as stated above.

5.4 Test subject

The testing on the voluntary test subject gave overall good results. The first electrogram test of the biopotential amplifier was a surface electromyography (sEMG) of the bicep. The preference was not to apply the electrodes for the first electrogram close to the heart, in case that anything was wrong with one of the electrodes, although the chance was very low considering the previous successful tests.

In some tests, the device needed about 10 to 15 seconds to get the output to its designed DC offset. In the case of powerline interference, without filtering of the MP35, an improvement in the noise reduction was seen, thanks to the driven right leg circuit. This circuit drove the common mode noise back to the body of the test subject, as designed.

Compared to an ECG, there is no expected shape in the output graph of the EMG. When the bicep is bent and immediately stretched back, a peak is shown at the output which is the expected result. When the bicep muscle is flexed, or continuously contracted, multiple peaks are the result. The sample rate of 1000 samples per second instead of 200 per second increased the noise. For this reason, RMS averaging was taken after the measurements to distinguish the contraction of the muscles. Filtering the data after the measurements appears to be a mandatory step in creating a useful EMG.

With the ECG it is possible to distinguish the P-wave, QRS-complex and T-wave of the heart signal. Sometimes the U-wave was detectable, but this was not always the case due to its low amplitude. The amount of noise was, in general for all electrograms, inconsistent. This was especially noticeable for the ECG because there is an expected signal pattern. One example is that placing an electrical device close to the PCB would result in an amplification of the noise seen at the output.

The EOG signal can detect the direction where the eyes of the test subject are looking. It is also possible to detect a difference in the angle the person is looking at. If there is a linear correlation between the angle of the eyes and the voltage amplitude, is not tested in this research.

At the moment of writing, taking an electroencephalogram with the biopotential amplifier has been unsuccessful. For testing, electrodes were placed on the forehead of the test subject with the reference electrode placed on the cheek. The electrodes were unable to detect brain activity but rather caught EOG signals. At the moment of writing, it is unclear if the PCB is unable to amplify the EEG signals or if the electrodes cannot catch the signals.

6 Conclusion

The single supply biopotential amplifier was designed and built on a printed circuit board after multiple simulations. The PCB was later tested using a bio simulator at the input that simulates a heart signal. The amplification of this signal was read on an Arduino Uno, an oscilloscope and the Biopac MP35.

The Arduino Uno is a viable option to read out the PCB output when using the bio simulator. Although it has a lower sample rate, the different waves of the ECG signal were distinguishable. The raw result on the oscilloscope was good with little noise. When averaging of the signal was applied all noise was removed which was even better. When using the built-in 50 Hz band stop of the Biopac MP35, a noise-free signal is displayed.

The ECG, EOG and EMG on a test subject using the Biopac MP35 was successful. Cleaning the signal after measurement was necessary for the EMG, but the ECG and EOG gave good results when a 50 Hz band stop was applied. The P-wave, QRS-complex, T-wave were distinguishable and sometimes even the U-wave was detectable. It was possible to determine the direction where the eyes were looking at while performing an EOG. However, performing an EEG was not possible with the use of these electrodes. For future research it can be interesting to determine if there is a linear correlation between the angle of the eyes and the voltage amplitude.

The improved PCB design should make it easier to connect the PCB to the Biopac MP35. Not only that, but using the headers makes it possible to power the PCB using a battery and readout the output using the pins. This new design should be tested further in future work. The design and building of a case around the PCB to block powerline interference and other noise is also recommended.

Bibliography

[1] M. Ubaid Hussein, “Electrical physics within the body,” 2018, p. 70.

[2] A. Friedman, A. Borisyuk, B. Ermentrout, and D. Terman, “Introduction to Neurons,” 2005, pp. 1–20. doi: 10.1007/978-3-540-31544-5_1.

[3] N. V. Thakor, “Biopotentials and Electrophysiology Measurement,” 1999.

[4] “Data Acquisition, Loggers, Amplifiers, Transducers, Electrodes | BIOPAC,” *BIOPAC Systems, Inc.* https://www.biopac.com/ (accessed Jun. 11, 2023).

[5] A. Salman, J. Iqbal, U. Izhar, U. S. Khan, and N. Rashid, “Optimized circuit for EMG signal processing,” in *2012 International Conference of Robotics and Artificial Intelligence*, Oct. 2012, pp. 208–213. doi: 10.1109/ICRAI.2012.6413390.

[6] M. A. Cavalcanti Garcia and T. M. M. Vieira, “Surface electromyography: Why, when and how to use it,” *Rev. Andal. Med. Deporte*, vol. 4, no. 1, pp. 17–28, Jan. 2011.

[7] A. Subasi, “Chapter 2 - Biomedical Signals,” in *Practical Guide for Biomedical Signals Analysis Using Machine Learning Techniques*, A. Subasi, Ed., Academic Press, 2019, pp. 27–87. doi: 10.1016/B978-0-12-817444-9.00002-7.

[8] “Signal Processing Techniques for Removing Noise from ECG Signals,” *jber*, Dec. 2019, doi: 10.17303/jber.2019.3.101.

[9] U. Satija, B. Ramkumar, and M. S. Manikandan, “A Review of Signal Processing Techniques for Electrocardiogram Signal Quality Assessment,” *IEEE Rev. Biomed. Eng.*, vol. 11, pp. 36–52, 2018, doi: 10.1109/RBME.2018.2810957.

[10] A. Kalyakulina *et al.*, “LUDB: A New Open-Access Validation Tool for Electrocardiogram Delineation Algorithms,” *IEEE Access*, vol. 8, pp. 186181–186190, Jan. 2020, doi: 10.1109/ACCESS.2020.3029211.

[11] F. Fang and T. Shinozaki, “Electrooculography-based continuous eye-writing recognition system for efficient assistive communication systems,” *PLOS ONE*, vol. 13, p. e0192684, Feb. 2018, doi: 10.1371/journal.pone.0192684.

[12] A. Bhandari, V. Khare, J. Santhosh, and S. Anand, “Wavelet based compression technique of Electro-oculogram signals,” in *IFMBE Proceedings*, 2007, pp. 440–443. doi: 10.1007/978-3-540-68017-8_111.

[13] N. V. Thakor and S. Tong, “Advances in Quantitative Electroencephalogram Analysis Methods,” *Annu. Rev. Biomed. Eng.*, vol. 6, no. 1, pp. 453–495, 2004, doi: 10.1146/annurev.bioeng.5.040202.121601.

[14] J. C. Huhta and J. G. Webster, “60-Hz Interference in Electrocardiography,” *IEEE Trans. Biomed. Eng.*, vol. BME-20, no. 2, pp. 91–101, Mar. 1973, doi: 10.1109/TBME.1973.324169.

[15] E. Spinelli, R. Pallas-Areny, and M. Mayosky, “AC-Coupled Front-End for Biopotential Measurements,” *IEEE Trans. Biomed. Eng.*, vol. 50, pp. 391–5, Apr. 2003, doi: 10.1109/TBME.2003.808826.

[16] A. Hambley, *Electrical Engineering: Principles & Applications, Global Edition*, 7th ed. New York: Pearson. Accessed: Mar. 16, 2023. [Online]. Available: https://www.pearson.com/store/p/electrical-engineering-principles-applications-global-edition/P200000004381/9781292223124

[17] “AC-coupling instrumentation amplifier improves rejection range of differential dc input voltage - EDN.” https://www.edn.com/ac-coupling-instrumentation-amplifier-improves-rejection-range-of-differential-dc-input-voltage/ (accessed Mar. 29, 2023).

[18] “The Art of Electronics Third Edition : Horowitz, Paul, Hill, Winfield: Amazon.es: Libros.” https://www.amazon.es/Art-Electronics-Third-Paul-Horowitz/dp/0521809266 (accessed May 21, 2023).

[19] O. Casas, E. M. Spinelli, and R. Pallas-Areny, “Fully Differential AC-Coupling Networks: A Comparative Study,” *IEEE Trans. Instrum. Meas.*, vol. 58, no. 1, pp. 94–98, Jan. 2009, doi: 10.1109/TIM.2008.927200.

[20] E. Spinelli and A. Veiga, “A fully-differential DC restoration circuit,” in *2016 IEEE 7th Latin American Symposium on Circuits & Systems (LASCAS)*, Feb. 2016, pp. 27–30. doi: 10.1109/LASCAS.2016.7451001.
[21] E. M. Spinelli, N. H. Martinez, and M. A. Mayosky, “A single supply biopotential amplifier,” *Med. Eng. Phys.*, vol. 23, no. 3, pp. 235–238, Apr. 2001, doi: 10.1016/S1350-4533(01)00040-6.
[22] E. Spinelli and F. Guerrero, “Chapter 12-THE BIOLOGICAL AMPLIFIER,” 2019. doi: 10.1142/10213.
[23] “Improving Common-Mode Rejection Using the Right-Leg Drive Amplifier,” 2011.
[24] R. P. Sallen and E. L. Key, “A practical method of designing RC active filters,” *IRE Trans. Circuit Theory*, vol. 2, no. 1, pp. 74–85, Mar. 1955, doi: 10.1109/TCT.1955.6500159.
[25] J. Baeten, *Systeemtheorie*. Katholieke Hogeschool Limburg, 2006.
[26] S. Grimnes and rjan G. ttem Martinsen, *Bioimpedance and Bioelectricity Basics*. Academic Press, 2000.
[27] “Nissha Medical Technologies | Healthcare Solutions.” https://uk.nisshamedical.com/ProdDescMed.aspx?pid=6000065C (accessed Jun. 04, 2023).
[28] “Medical ECG Electrode Adapter Cable Angle Plug Manufacturers and Suppliers - Factory Price - Pray-Med Technology,” *Shenzhen Pray-Med Technology Co.,Ltd*. https://www.pray-med.com/ecg/one-piece-ecg-cable/medical-ecg-electrode-adapter-cable-angle.html (accessed Jun. 05, 2023).
[29] “MP35 Four Channel Data Acquisition System.” BIOPAC Systems, Inc., Aug. 2017. [Online]. Available: https://www.biopac.com/wp-content/uploads/MP35.pdf
[30] “BSL HARDWARE GUIDE.” BIOPAC Systems, Inc., Sep. 2016.
[31] “Full/Low Speed 2.5 kV USB Digital Isolator ADuM3160.” Analog Devices, Feb. 2010. [Online]. Available: https://www.analog.com/media/en/technical-documentation/data-sheets/ADuM3160.pdf
[32] “The Full Arduino Uno Pinout Guide [including diagram],” *circuito.io blog*, Aug. 12, 2018. https://www.circuito.io/blog/arduino-uno-pinout/ (accessed Jun. 07, 2023).
[33] “TINA-TI Simulation tool | TI.com.” https://www.ti.com/tool/TINA-TI (accessed Jun. 12, 2023).
[34] B. B. Winter and J. G. Webster, “Driven-right-leg circuit design,” *IEEE Trans. Biomed. Eng.*, vol. BME-30, no. 1, pp. 62–66, Jan. 1983, doi: 10.1109/TBME.1983.325168.
[35] “TLC227x, TLC227xA: Advanced LinCMOS Rail-to-Rail Operational Amplifiers.” Texas Instruments, Mar. 2016. [Online]. Available: https://www.ti.com/lit/ds/symlink/tlc2274a.pdf?ts=1685879010543&ref_url=https%253A%252F%252Fwww.ti.com%252Fproduct%252FTLC2274A%252Fpart-details%252FTLC2274ACN%253Futm_source%253Dgoogle%2526utm_medium%253Dcpc%2526utm_campaign%253Docb-tistore-promo-asc_opn_en-cpc-storeic-google-wwe%2526utm_content%253DDevice%2526ds_k%253DTLC2274ACN%2526DCM%253Dyes%2526gclid%253DCjwKCAjwyeujBhA5EiwA5WD7_ROWXdnbXMF_L2atGdEZe7w-E8P1nmlHdRIYf8tos91XmZhcWXNeFBoCYCEQAvD_BwE%2526gclsrc%253Daw.ds
[36] “PCB Trace Width Calculator - PCB Prototype the Easy Way - PCBWay.” https://www.pcbway.com/pcb_prototype/trace-width-calculator.html (accessed Jun. 05, 2023).
[37] megcircuitsprojects, “EMG Sensing Circuit,” *Instructables*. https://www.instructables.com/EMG-Sensing-Circuit/ (accessed Jun. 07, 2023).
[38] M. Cadogan, “ECG Lead positioning,” *Life in the Fast Lane • LITFL*, May 20, 2021. https://litfl.com/ecg-lead-positioning/ (accessed Jun. 07, 2023).
[39] R. Weir and G. Frantz, “Guidelines for Using Decoupling Capacitors on DSP Designs”.

Appendices list

Appendix A. Electronic schematic of EMG in TINA TI ……65
Appendix B. Electronic schematic of EOG in TINA TI ……65
Appendix C. Electronic schematic of EEG in TINA TI ……..65
Appendix D. Front side of 3D render of the combined PCB design without components……66
Appendix E. Back side of 3D render of the combined PCB design without components……..67

Appendices

Appendix A. Electronic schematic of EMG in TINA TI

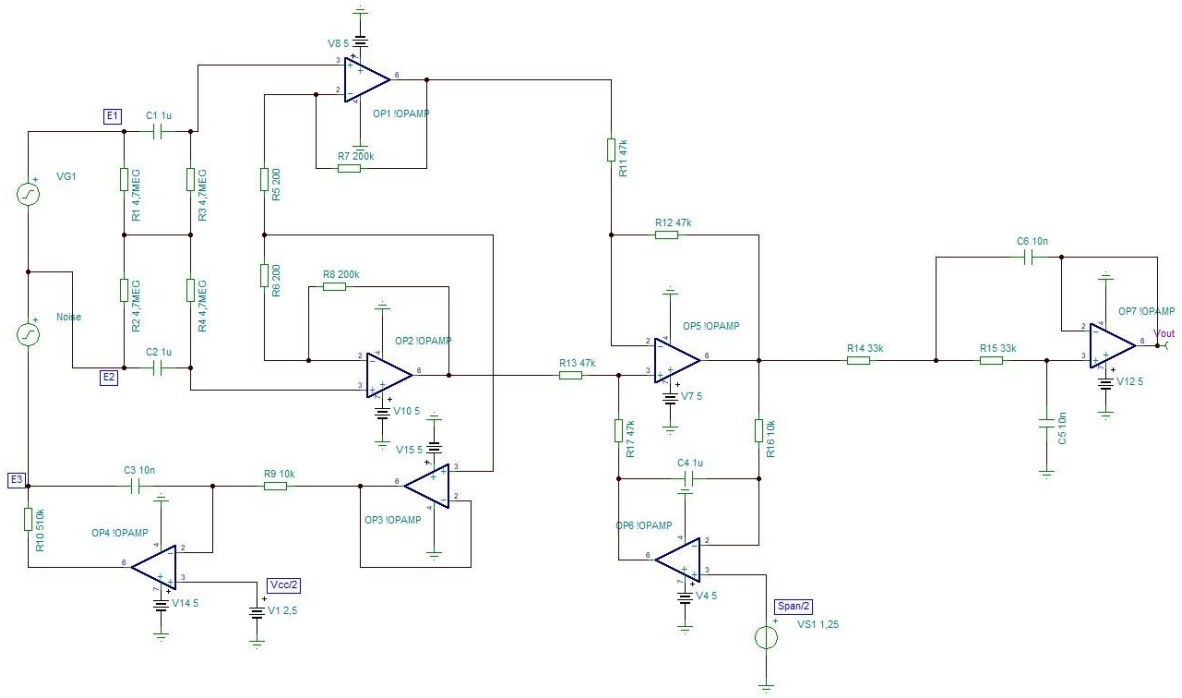

Appendix B. Electronic schematic of EOG in TINA TI

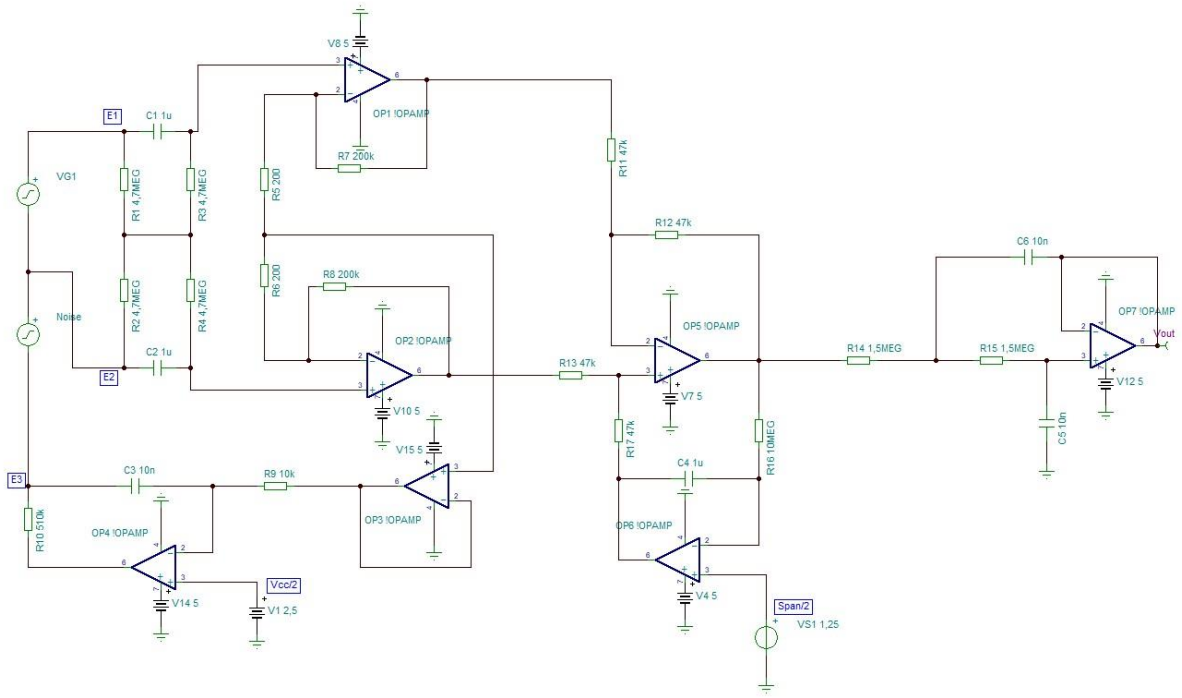

Appendix C. Electronic schematic of EEG in TINA TI

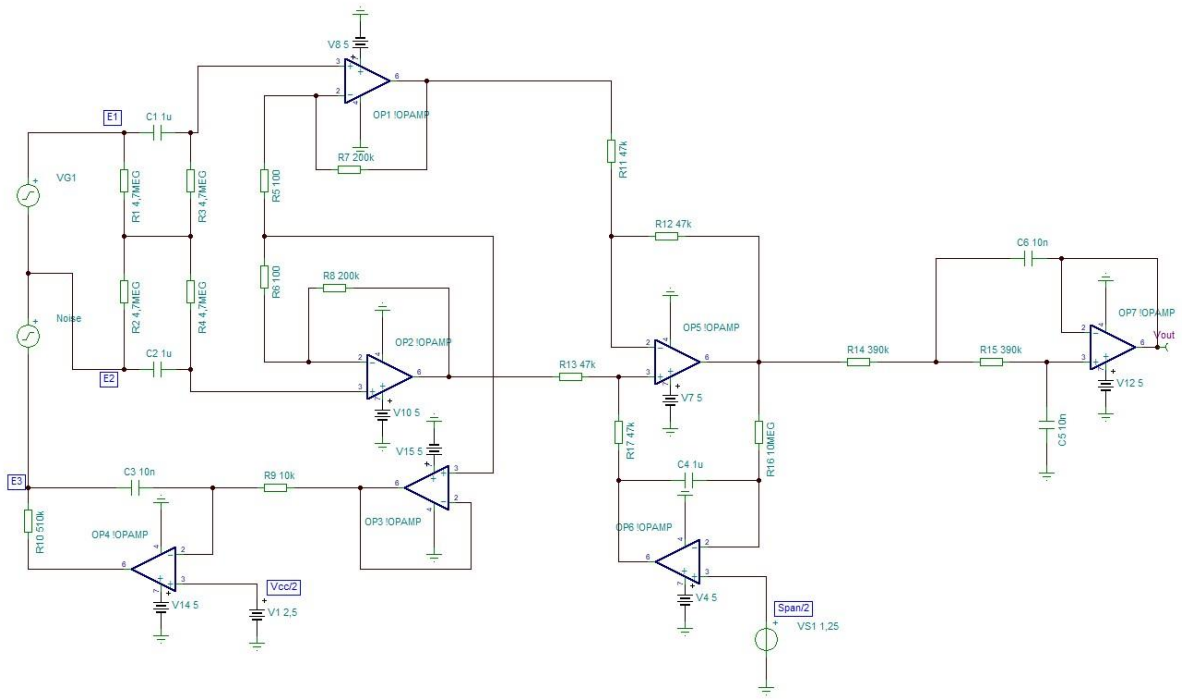

Appendix D. Front side of 3D render of the combined PCB design without components

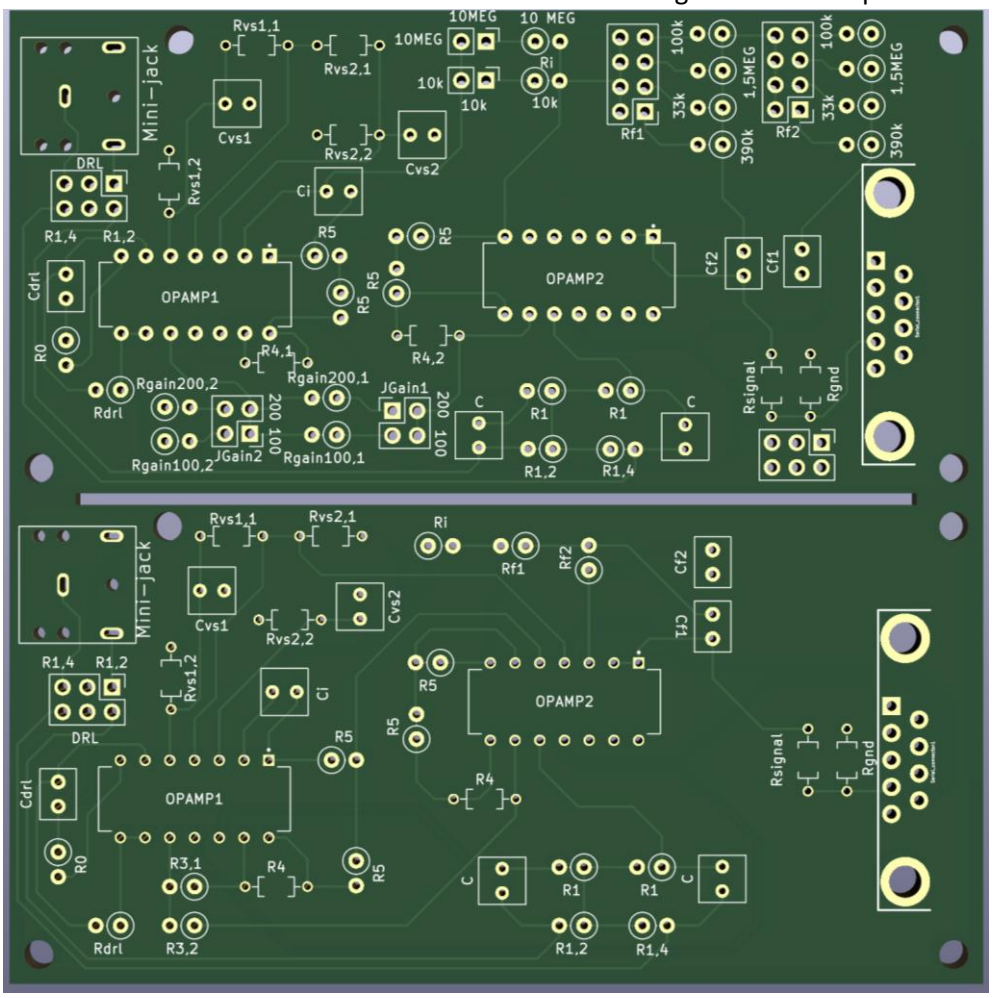

Appendix E. Front side of 3D render of the Combined PCB design without components.